



저작자표시-변경금지 2.0 대한민국

이용자는 아래의 조건을 따르는 경우에 한하여 자유롭게

- 이 저작물을 복제, 배포, 전송, 전시, 공연 및 방송할 수 있습니다.
- 이 저작물을 영리 목적으로 이용할 수 있습니다.

다음과 같은 조건을 따라야 합니다:



저작자표시. 귀하는 원저작자를 표시하여야 합니다.



변경금지. 귀하는 이 저작물을 개작, 변형 또는 가공할 수 없습니다.

- 귀하는, 이 저작물의 재이용이나 배포의 경우, 이 저작물에 적용된 이용허락조건을 명확하게 나타내어야 합니다.
- 저작권자로부터 별도의 허가를 받으면 이러한 조건들은 적용되지 않습니다.

저작권법에 따른 이용자의 권리는 위의 내용에 의하여 영향을 받지 않습니다.

이것은 [이용허락규약\(Legal Code\)](#)을 이해하기 쉽게 요약한 것입니다.

[Disclaimer](#)

碩士學位論文

Study of Physicochemical
property of ethosome in
accordance with ceramide and
characteristics of drug

濟州大學校 大學院

化 學 科

현 통 일

2022年 2月



Study of Physicochemical
property of ethosome in
accordance with ceramide and
characteristics of drug

指導教授 尹 景 燮

玄 統 一

이 論文을 理學 碩士學位 論文으로 提出함

2022年 2月

玄 統 一의 理學 碩士學位 論文을 認准함

審査委員長 _____ (印)

委 員 _____ (印)

委 員 _____ (印)

濟州大學校 大學院

2022年 2月

Study of Physicochemical property of
ethosome in accordance with ceramide and
characteristics of drug

Tong-Il Hyeon

(Supervised by Professor Kyung-Sup Yoon)

A thesis submitted in partial fulfillment of the
requirement for the degree of Master of Science

2022. 2.

This thesis has been examined and approved.

.....
.....
.....
.....
Date

Department of Chemistry
GRADUATE SCHOOL
JEJU NATIONAL UNIVERSITY

Contents

List of Tables	iii
List of Figures	iv
Abstract	vi
I. Introduction	1
II. Materials and Methods	11
2.1. Materials	11
2.2. Preparation of primary ethosome	12
2.3. Preparation of nano-sized ethosome	16
2.4. Measurement of particle size and polydispersity index	16
2.5. Measurement of zeta potential	17
2.6. Franz diffusion cell experiment of nano-sized ethosome	17
2.7. Encapsulation efficiency of nano-sized ethosome	20
2.8. Drug release of nano-sized ethosome	21
2.9. Image of cryo transmission electron microscope	23
2.10. Statistical analysis	23
III. Results & Discussion	24
3.1. Physicochemical properties of nano-sized ethosome	24

3.1.1. Particle size and polydispersity index of nano-sized ethosome in line with ceramide	27
3.1.2. Zeta potential of nano-sized ethosome in line with ceramide . . .	31
3.1.3. Particle size and polydispersity index of nano-sized ethosome over time	37
3.1.4. Zeta potential of nano-sized ethosome over time	41
3.2. Skin absorption efficiency of nano-sized ethosome	43
3.3. Encapsulation efficiency of nano-sized ethosome	47
3.4. Drug release of nano-sized ethosome	49
3.5. Cryo-TEM image of nano-sized ethosome	54
IV. Summary & Conclusion	58
V. Acknowledgement	60
VI. Reference	61

List of Tables

Table 1. Feature of drugs	9
Table 2. The weight percent of oil and water part in vanillic acid ethosome	13
Table 3. The weight percent of oil and water part in α -Bisabolol ethosome	14
Table 4. Method of vanillic acid and α -Bisabolol for HPLC with PDA detector	19
Table 5. Appearance, particle size, polydispersity index, zeta potential of VAE, and ABE	26
Table 6. Particle size of VAE and ABE over time	34
Table 7. Polydispersity index of VAE and ABE over time	35
Table 8. Zeta potential of VAE and ABE over time	36
Table 9. Skin absorption efficiency of VAE	45
Table 10. Skin absorption efficiency of ABE	46
Table 11. Encapsulation efficiency of VAE	51
Table 12. Encapsulation efficiency of ABE	51
Table 13. Drug release of VAE by dialysis membrane method	51
Table 14. Drug release of ABE by dialysis membrane method	51

List of Figures

Figure 1. Skin structure of human being	2
Figure 2. Mechanism of skin absorption	3
Figure 3. How to be formed liposome from phospholipid	5
Figure 4. Chemical structure of vanillic acid, (-) - α - Bisabolol and ceramide NP	7
Figure 5. Preparation of ethosome by high pressure homogenization method	15
Figure 6. Dialysis membrane method for drug release	22
Figure 7. Appearance of VAE #1~6 at 25°C after a day and 4 weeks	25
Figure 8. Appearance of ABE #1~6 at 25°C after a day and 4 weeks	25
Figure 9. Particle size of VAE and ABE at 25°C after a day	29
Figure 10. Polydispersity index of VAE and ABE at 25°C after one day	30
Figure 11. Zeta potential of VAE and ABE at 25°C after one day	33
Figure 12. Particle size of VAE and ABE at 25°C over time	39
Figure 13. PDI of VAE and ABE at 25°C over time	40
Figure 14. Zeta potential of VAE and ABE at 25°C over time	42
Figure 15. Skin absorption efficiency of VAE and ABE at 37°C \pm 1	46
Figure 16. Drug release of VAE and ABE at 37°C \pm 1 by dialysis membrane method for 72 h	52
Figure 17. Drug release of VAE and ABE at 37°C \pm 1 by dialysis membrane	

method for 12h	53
Figure 18. Cryo-TEM image of VAE #6	56
Figure 19. Cryo-TEM image of ABE #6	57

Abstract

Study of physicochemical property of ethosome in accordance with ceramide and characteristics of drug

화장품 산업에서 생리활성 물질을 효과적으로 전달하기 위하여 다양한 제형이 이용되고 있다. 그 중 효과적이라고 알려진 리포솜 제형을 이용하여 세라마이드와 바닐산 또는 알파-비사보롤을 함유한 인지질 이중층 소포체의 물리화학적 특성을 연구하였다. 약물은 크게 두 가지 종류가 쓰였는데 바닐산은 친수성 약물로서 에토솜의 중앙 수상 부분에 포집되며 알파-비사보롤 경우는 친지질성 약물로서 이중층 구조에 포집이 되게 된다. 세라마이드와 바닐산을 함유한 에토솜의 입자크기 범위는 80 ~ 130 nm 이고, 반면에 세라마이드와 알파-비사보롤을 함유한 경우 150 ~ 170 nm 의 크기를 갖는다. 바닐산을 함유한 에토솜에서 세라마이드 함량 변화를 주면 입자크기가 작아 졌고 알파-비사보롤을 함유한 에토솜의 입자크기는 큰 변화가 없었다. 4주간 25℃, 4℃, 그리고 45℃에서 안정성을 확인한 결과를 보면, 세라마이드와 약물을 동시에 포집하여도 안정성을 유지하는 것을 관찰하였다. 세라마이드를 함유한 바닐산 에토솜과 대조군의 피부흡수율을 관찰한 결과, 세라마이드를 함유한 바닐산 에토솜의 피부흡수율이 24시간 동안 약 15% 증가하는 것을 확인하였다. 하지만, 알파-비사보롤의 경우는 세라마이드가 있는 에토솜의 피부흡수율이 대조군 보다 미세하게 높았다. 추가적으로, 캡슐효율, 약물방출, cryo-TEM 이미지를 측정하였다. 본 연구 결과들을 바탕으로, 세라마이드와 약물을 동시에 포집한 에토솜과 다른 화장품 제형과 접목하여서 화장품 산업에서 쓰일 것으로 사료된다.

In the cosmetic industries, numerous formulations have been utilized to delivery effectively bioactive ingredients. By selecting liposome formulation that is well-known among them, bilayer lipid vesicles composed of ceramide and vanillic acid or α -Bisabolol were prepared and their physicochemical properties studied. Ethosomes were loaded with either hydrophilic vanillic acid or lipophilic α -Bisabolol. Vanillic acid was encapsulated in the aqueous core, while α -Bisabolol was interdigitated with the lipid phase. The range of particle size of ethosome with ceramide and vanillic acid were 80 ~ 130 nm, while which of ethosome with ceramide and α -Bisabolol were 150 ~ 170 nm. Increasing the quantity of ceramide in ethosome with vanillic acid reduced the particle size, and the size of α -Bisabolol ethosome was not nearly changed. The stability of both ethosomes did not change sharply for 4 weeks at 25°C, 4°C and 45°C. Skin absorption efficiency of ceramide vanillic acid ethosomes was increased by approximately 15% compared with control, whereas ethosome containing α -Bisabolol and ceramide was slightly higher than control. Further, encapsulation efficiency, drug release were measured, and cryo-TEM were collected. Based on the study results, we propose that ceramide containing ethosomes could be utilized in the cosmetic industry by grafting with a wide range of other cosmetic formulations.

I. Introduction

The cosmetics and pharmaceutical industries face challenges in the delivery of bioactive drugs to the body. The medium used to deliver drugs might be vulnerable to external stress and be broken down before delivery can occur. Moreover, drugs might be able to react with other materials during transport to the target area. The skin presents a crucial obstacle for drugs to be delivered by transdermal systems. [1] The skin system is composed of epidermis, dermis, and fatty tissue (Fig 1). Drug absorption through the stratum corneum of the epidermis occurs by three routes: intercellular, transcellular or appendageal (Fig 2). The transcellular route of drug transport involves passing through a relatively hydrophilic environment and highly lipophilic intercellular lipid matrix. The intercellular route involves passing through the intercellular lipids. Meanwhile, the appendageal mechanism of drug transport involves passage through sweat glands and hair follicles. Traditional cosmetic formulations are poorly able to transport bioactive substances deep into the skin due to the difficulty of passing the stratum corneum and damage from external factors. [2, 3] There are numerous approaches being researched to overcome these challenges. One approach is the use of liposomes that encapsulate active agents for delivery to target areas via the intercellular route.

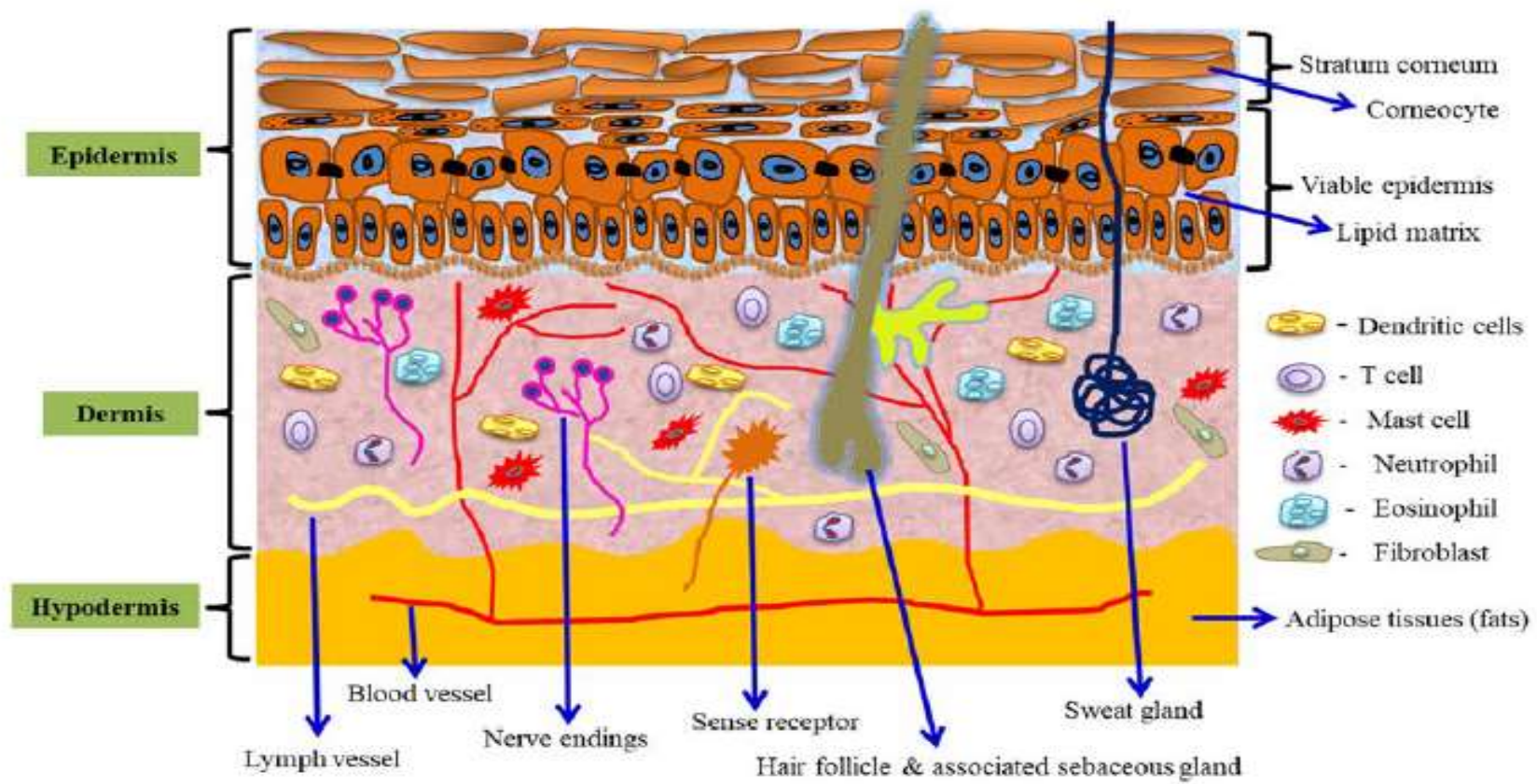


Fig 1. Skin structure of human being [28]

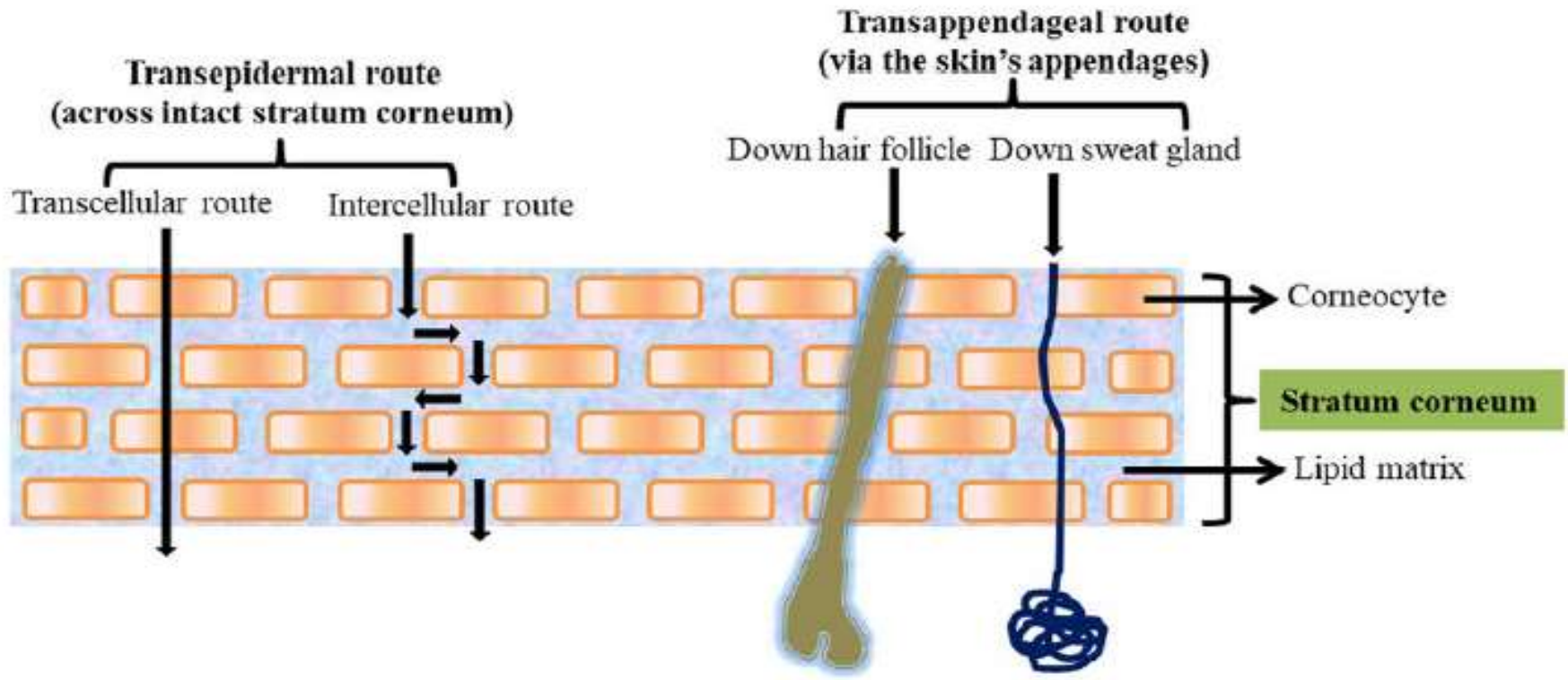


Fig 2. Mechanism of skin absorption [28]

Liposomes can deliver drugs in a concentration–dependent manner across the stratum corneum. Multilamellar vesicles (MLV) are a type of vesicle that can deliver active ingredients to the stratum corneum, epidermis, and dermis, insignificantly higher concentrations than classical topical formulations, e.g. creams, lotions, gels, or emulsions. [4]

Liposomes were first created by British hematologist Dr. Alec D Bangham who made multilamellar vesicle through lecithin by thin film hydration method. [5] Liposomes can be prepared using phospholipids. In aqueous media, these form bilayer structures and subsequently spherical liposomes. Liposomes are prepared using phospholipid and cholesterol, which are components of human skin, and thus are inherently biocompatible and biodegradable. Liposomes are amphipathic as phospholipid has both a hydrophilic phosphate head group and a lipophilic fatty–acid chain tail group. Cholesterol plays a critical role in the stability of the liposome bilayer membrane. [6, 7] Drugs can be encapsulated in the aqueous core or bilayer structure to be delivered to desired targets. [8]

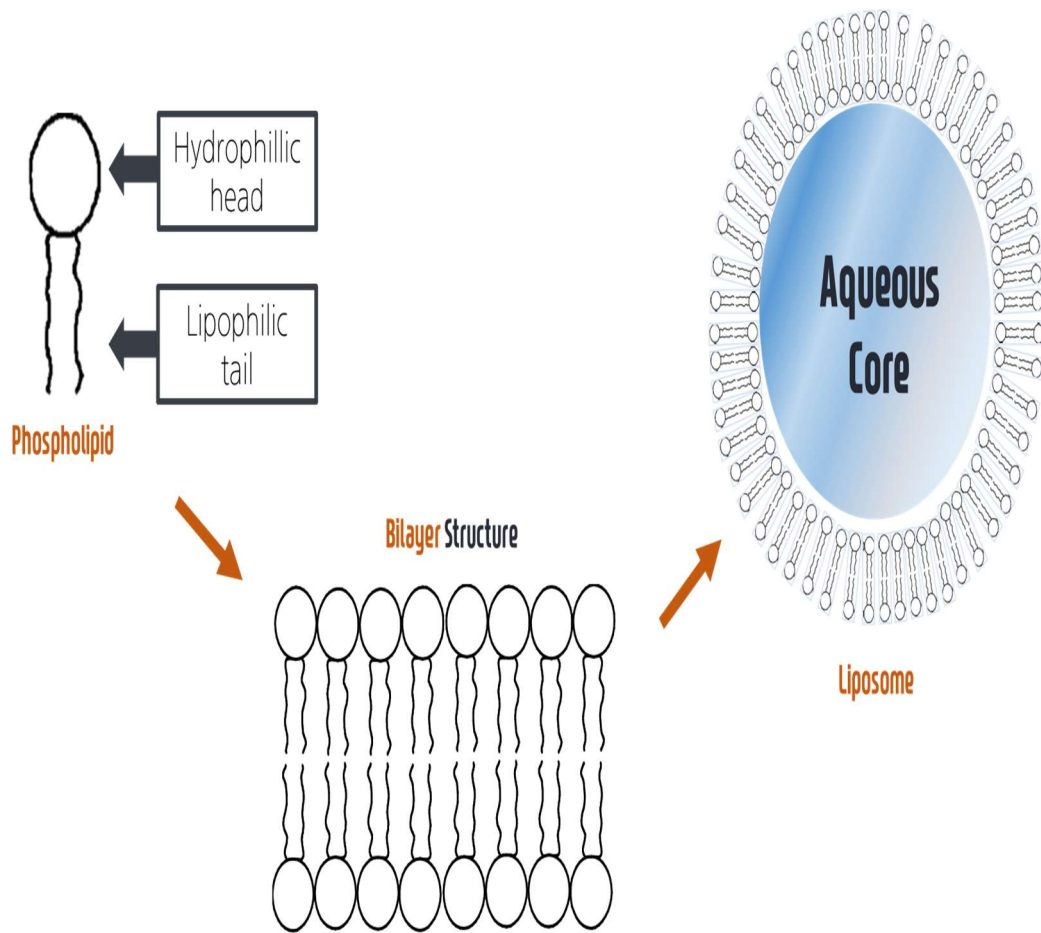
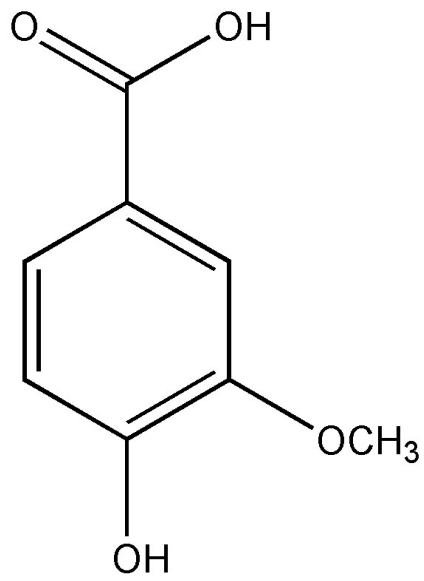
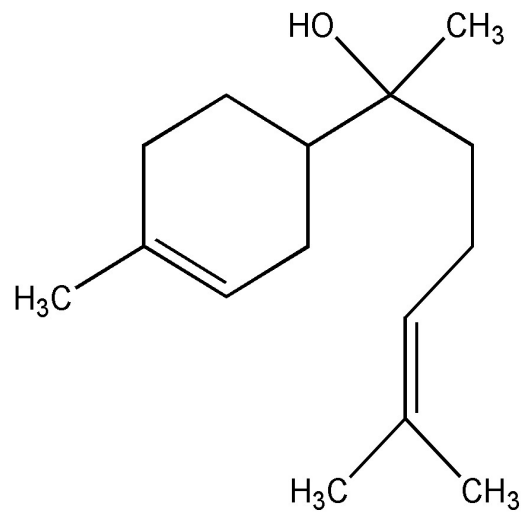


Fig 3. How to be formed liposome from phospholipid.

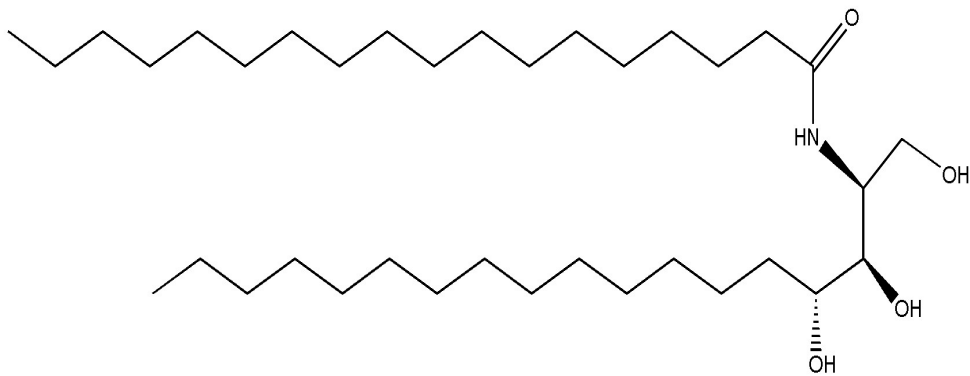
When preparing liposomes by the traditional thin film hydration method, organic solvents are used and an additional step to remove the solvent by evaporation is required. This adds to the time taken for preparation and residual organic solvents may pose risks to health. Moreover, the organic solvents may degrade the active ingredients releasing chemicals, which could be hazardous to human health. [9] In order to overcome those limitations, one can utilize another relatively safe dispersion medium like ethanol compared to organic solvents such as methanol or chloroform. This method utilizing ethanol to produce lipid vesicles composed of ethanol, phospholipids, and water was created by Touitou. [10] Liposomes created using ethanol are called ethosomes. Ethosomes have a more flexible bilayer structure than liposomes prepared by traditional thin film method because of residual ethanol in the bilayer. The vesicles have higher skin absorption efficiency thanks to this flexible bilayer structure. [11]



Vanillic acid



(-)- α -Bisabolol



Ceramide NP

Fig 4. Chemical structure of vanillic acid, (-)- α -Bisabolol and ceramide NP

In this study, several types of drug were used. α -bisabolol, a monocyclic sesquiterpene alcohol, is a lipophilic drug first extracted from the flowers of chamomile in 1951. [12] α -Bisabolol has a weak floral odor and has anti-inflammatory, antibacterial, antiseptic, and antioxidant activities. In addition, it has been used to protect skin from external stress in formulations such as body lotion, sun care and baby care products. [13] Vanillic acid (4-hydroxy-3-methoxybenzoic acid) is hydrophilic drug and a phenolic derivative of edible plants and fruits. It has antibacterial and antimicrobial effects and is an effective anti-inflammatory for colitis. It exhibits anticancer properties in experimentally induced carcinogenesis and can serve as a hair loss prevention agent. [14-16]

Ceramide is a complex of fatty acid that is combined with the amide of a sphingoid base. Ceramide in human skin is categorized in 12 groups according to the esterification of 4 types of sphingoid base as well as 3 types of fatty acids. Intercellular lipid mass is composed of 50 % ceramides, and these play an important role in repairing dermal damage. Ceramides have been utilized as raw materials for cosmetics, and for the treatment of skin damage and aging. [17] Exogenous application of emollients or lipid mixture with ceramide improves and recover damaged dermal function. In patients who have atopic dermatitis and poor skin barrier function, administration of ceramide-containing emollient led to significantly improved skin barrier function after 21 weeks. [18, 19]

Table 1. Feature of drugs

Drug	Vanillic acid	α -Bisabolol	Ceramide NP
Activate effect	antibacterial antimicrobial hair loss prevention	anti-inflammatory antibacterial antiseptic antioxidant	Improving and recovering dermal function
Appearance	yellowish brown powder	transparent liquid	white powder
Odor	vanilla flavor	a weak floral odor	odorless

Ethosomes are prepared by a high pressure homogenization method. Passing ethosomes through a high pressure homogenizer, ensures small particle size and a narrow polydispersity index. The main purpose of nano-disperser converts multilamellar to unilamellar vesicles. The underlying fluid mechanics involved in this preparation of ethosomes are impact, shear force, and cavitation. Impact is literally collision between vesicles and the wall of the chamber in the nano-disperser. Shear force is an action generated by the difference in flow velocity between the center of the tube and the edge of the tube of fluid flowing in the chamber. According to Bernoulli's law, the static pressure in a fluid is decreased at high flow velocity. Bubbles filled with steam or gas arise and grow until elevation of the pressure causes their implosion, provided that the local pressure is below the steam pressure. The surrounding water and lipid bilayers are accelerated towards the middle of the bubble followed by shock waves. This causes high local stress, e.g. tearing into parts of the bilayer and excavation of the steel surface. [20, 21]

In the present work based on previous research [22], the physicochemical properties of ethosomes were compared in accordance with characteristics of drugs as well as ceramide. The stability, skin absorption efficiency, encapsulation efficiency, drug release, and cryo-TEM image of ethosomes containing hydrophilic or lipophilic drugs in addition to ceramide was studied.

II. Materials and Methods

2.1 Materials

Hydrogenated lecithin (Lipoid S75-3, Lipoid GmbH, Germany), used as a surfactant, was purchased from Lipoid GmbH (Ludwigshafen, Germany). Cholesterol (Cholesterol JP, Nippon Fine Chemical Co. LTD, Japan), ceramide NP (DS-Ceramide Y30, Doosan Solus Advanced Materials, Korea), ethanol (Ethanol anhydrous (95~96%) Daejung, Korea), vanillic acid (Vanillic acid, Sigma-Aldrich, USA), α -Bisabolol((-)- α -Bisabolol, Sigma-Aldrich, USA) and arginine (L-Arginine, Ajinomoto, Japan) were used. PEG-60 hydrogenated castor oil (HCO 60, Kao Corporation, Japan) was used as a solubilizing agent for (-)- α -Bisabolol in control. Water (Deionized water (< 0.1 μ S/cm)) was manufactured by instrument (EXL1 Analysis, Vivagen, Korea). Ethylhexylglycerin (Saskine 50, Sachem Corporation, USA) was used as well. All other chemicals not mentioned were analytical grade.

2.2 Preparation of primary ethosome

For preparing primary vanillic acid ethosomes and α -Bisabolol ethosomes, Hydrogenated lecithin, cholesterol, ceramide NP and ethanol were weighed into a beaker (the oil phase). Meanwhile, they and α -Bisabolol were weighed into other beakers for α -Bisabolol ethosomes. Vanillic acid, arginine, ethylhexylglycerin, and water (water phase) were weighed in to beakers for vanillic acid ethosomes. A control was prepared in the same manner with the omission of ceramide. A summary of the assessed formulations is shown in Tables 1 and 2.

The weighed beakers of the water phase and oil phase were heated at 70–75°C. The oil part was added into the water part slowly and the mixed material emulsified at 2,800–3,100 rpm for 5 min using a homogenizer (Homogenizing mixer Mark II Model 2.5, PRIMIX, Japan). The primary vanillic acid ethosomes and α -Bisabolol ethosomes were cooled at 40–45°C and air bubble in the ethosomes were eliminated by defoaming instrument (Eyela A-1000S, Eyela, Japan). The following were also used: ethosomes with vanillic acid (VAE), ethosomes with α -Bisabolol (ABE), and ceramide (CR).

Table 2. The weight percent of oil and water part in vanillic acid ethosome.

	Materials	VAE #1	VAE #2	VAE #3	VAE #4	VAE #5	VAE #6	VAE Control
Oil Part	Hydrogenated Lecithin	1.5						—
	Cholesterol	0.5						—
	Ceramide NP	—	—	0.15	0.3	0.45	0.6	—
	Ethanol	15.0						
Water Part	Vanillic acid	—	0.1					
	Arginine	0.06						
	Ethylhexylglycerin	0.1						
	Water	to 100						

Table 3. The weight percent of oil and water part in α -Bisabolol ethosome.

Materials		ABE #1	ABE #2	ABE #3	ABE #4	ABE #5	ABE #6	ABE Control
Oil Part	Hydrogenated Lecithin	1.5						–
	PEG-60 Hydrogenated Castor Oil	–	–	–	–	–	–	1.5
	Cholesterol	0.5						–
	(-)- α -Bisabolol		0.5					
	Ceramide NP	–	–	0.15	0.3	0.45	0.6	–
	Ethanol	15.0						
Water Part	Ethylhexylglycerin	0.1						
	Water	to 100						

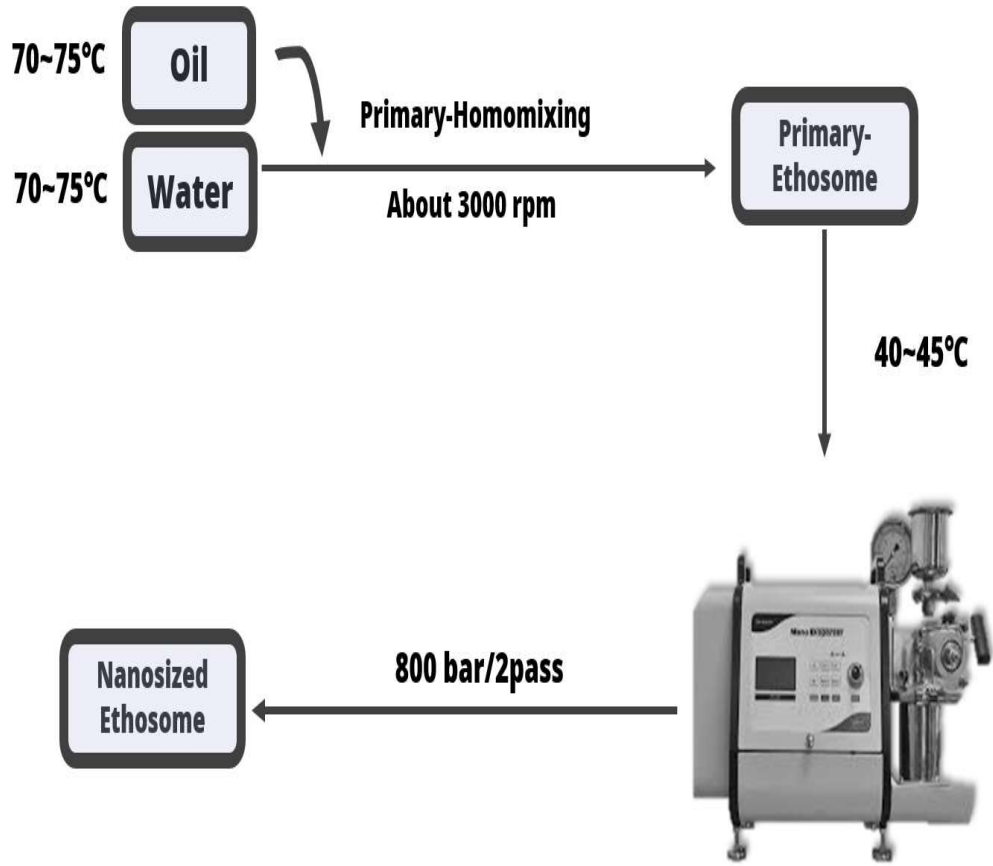


Fig 5. Preparation of ethosome by high pressure homogenization method

2.3 Preparation of nano-sized ethosome

The ethosomes described in section 2.2 were passed twice at 800 bar in a high-pressure nanodisperser (NLM 100, Ilshin Autoclave, Korea). When the vesicles passed nanodisperser, particles were shrunk and the polydispersity index was narrowed due to impact, shear force, and cavitation. The nano-sized ethosomes were stored at 4, 25, or 45 °C for 4 weeks.

2.4 Measurement of particle size and polydispersity index

The particle size and polydispersity index (PDI) of ethosomes were evaluated by dynamic light scattering (DLS) in the sub-micron range. [23, 24] The ethosomes were diluted to 10 % by water in a vial. The diluted samples were mixed for 30 s using a vortex instrument (Vortex Genie 2, Scientific Industries, Bohemia). Cells of the zetasizer were filled with ethosome suspension. The particle size and PDI of diluted samples were measured in the nano-zetasizer (Nano-ZS, Malvern Panalytical, England) at 25°C. Its software program was Zetasizer software and the Stokes-Einstein equation was used in the measurement of both particle size and PDI.

2.5 Measurement of zeta potential

The zeta potential was measured in the nano-zetasizer (Nano-ZS, Malvern Panalytical, England) at 25°C. Each 10% diluted samples was put into the zetasizer cell. The software of the instrument was Zetasizer software and the data processing was conducted using Smoluchowski's equation.

2.6 Franz diffusion cell experiment of nano-sized ethosome

The skin absorption efficiency of vanillic acid or α -Bisabolol was assessed by Franz diffusion-cell experiment. The Franz cell diffusion is processed by DHC-6TD (Logan Instruments, USA). A mixture of 50% ethanol (ethanol: water = 1:1 (v/v)) was filled into the receptor part of the Franz diffusion cell instrument. Artificial skin membranes (Strat-M membrane 25 mm discs, Merck Millipore, USA) were mounted onto Franz diffusion cells and the donor part was put above the receptor part at 37 ± 1 °C. In order to mix adequately, the receptor part was stirred with a magnetic bar at 300 rpm. Next, 400 μ l of ethosome sample was applied on the skin membrane and allowed to spread over the membranes. The solution in the receptor parts was taken for analysis after 1, 2, 4, 8, 12, and 24 h, respectively. [25] The donor parts were withdrawn and diluted with methanol (10 ml). Each skin membrane was cut into 8 pieces and each part was put into a conical tube with 10 ml methanol. Remaining donor and

receptor samples were sonicated for 1 h (Ultrasonic cleaner JAC-3010, Kodo, Japan) to destroy the bilayer structure of the ethosomes. All samples were analyzed by HPLC (2695, Waters, USA) equipped with PDA detector (2998, Waters, USA). The HPLC method was illustrated in the Table 4.

Table 4. Method of vanillic acid and α -Bisabolol for HPLC with PDA detector

System	Condition				
	Vanillic acid		α -Bisabolol		
Column	Kromasil C18 column, 5 μ m, 4.6 \times 250 mm (AkzoNobel, Netherlands)				
Temperature of column and sample	40 $^{\circ}$ C and 25 $^{\circ}$ C				
Mobile phase	A: 0.1% Acetic acid B: Methanol	0 m	A : 75 B : 25	A : Acetonitrile B : 0.1% Acetic acid	A : 80 B : 20
		30 m	A : 50 B : 50		
Flow rate	1.0 mL/min				
Injection volume	10 μ L				
Detector	Photodiode Array				
Wavelength	260 nm		210 nm		

2.7 Encapsulation efficiency of nano-sized ethosome

The method of asseing encapsulation efficiency was taken from H. J. Gwak et al[26], and C. K. Kim[27]. The ethosome samples were centrifuged (21,000 x g, 4°C, 3 h) by ultracentrifuge instrument (Varispin 15R, multi centrifuge, Novapro, Korea) to evaluate encapsulation efficiency of vanillic acid and α -Bisabolol in the ethosome. After separating the ethosomes into supernatant and lower layer, 100 μ L of the free drug layer of each was sampled. Each samples was diluted with 10 mL methanol and sonicated for 3 min. These were analyzed by HPLC by the method shown in the Table 3. The encapsulation efficiency of ethosomes was calculated as follows:

$$EE (\%) = \frac{C_T - C_U}{C_T} \times 100$$

where C_U is the amount of free drug in the ethosome sample, and C_T is the amount of total drug in the ethosome sample.

2.8 Drug release of nano-sized ethosome

Drug release of vanillic acid or α -Bisabolol was verified by dialysis membrane method. Before doing the experiment, dialysis tube (Spectra/Por[®] Dialysis Membrane, 300 kD, Spectrum laboratories, Inc., USA) was dipped in ultrapure water for 30 min prior to use. There were two types of solutions utilized for drug release. Type 1 solution for vanillic acid was NaCl:PBS:Water = 0.9:10:89.1 (w/w). Type 2 solution for α -Bisabolol was NaCl:PBS:polysorbate 20:Water = 0.9:10:1:88.1 (w/w). A beaker was filled with 200 mL prepared type 1 or type 2 solution. Ethosome samples (2 mL) were put into the soaked dialysis tube, and the tube was closed (Dialysis tubing closures, size 50 mm, Sigma-Aldrich, USA). The dialysis tube was put into the beaker and was stirred at 200 rpm at 37 °C \pm 0.5. At 1, 2, 4, 8, 12, 24, 48, and 72 h, 2 mL solution in the beaker was sampled and replenished with 2mL prepared solution. The sample solutions were diluted with 2 ml MeOH. The quantity of drug after dialysis was calculated by HPLC shown in Table 4.

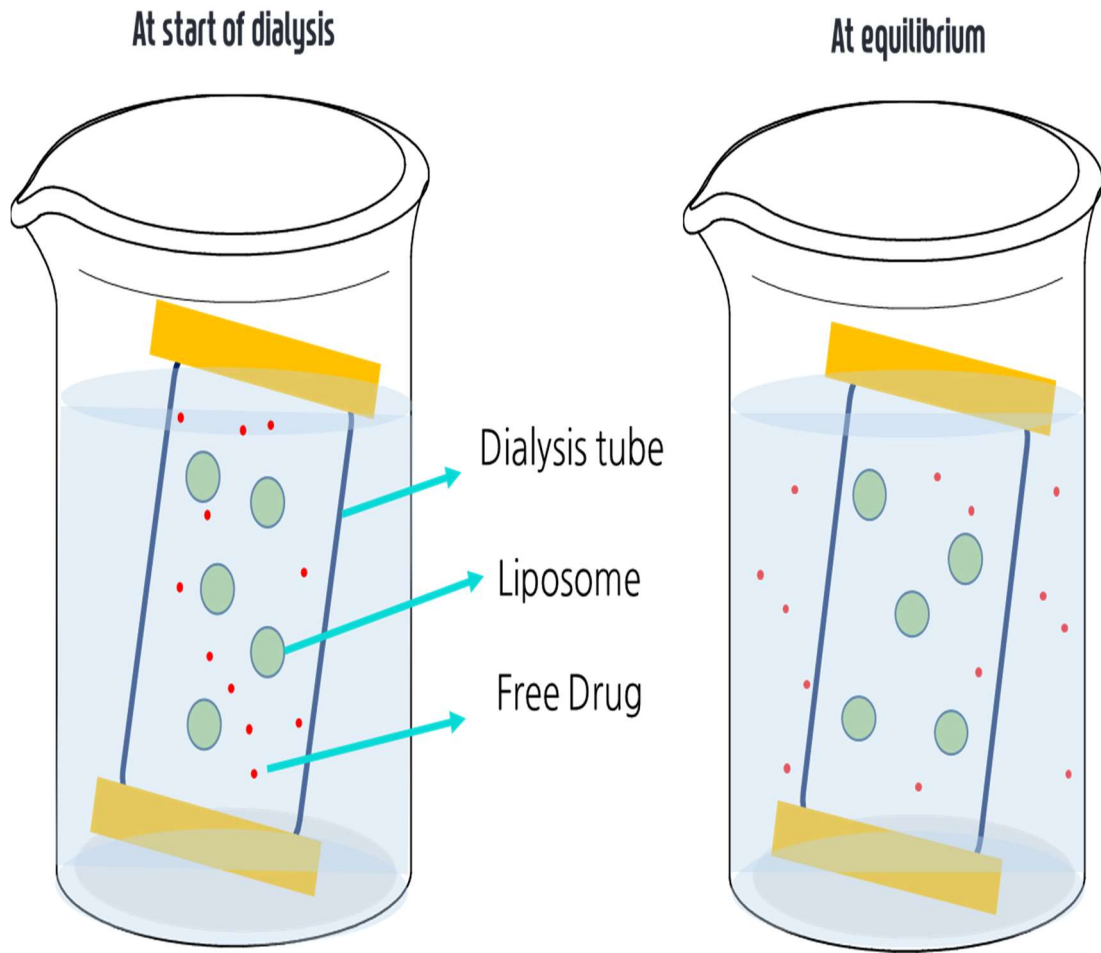


Fig 6. Dialysis membrane method for drug release

2.9 Image of cryo transmission electron microscope

In order to verify vesicle shape, cryo-TEM imaging of vesicles was performed by an outside agency (KIST, Korea Institute of Science and Technology, Korea), as Jeju National University is not equipped with a cryo-TEM facility. The Cryo-TEM model was FEI Tecnai F20 G² (Thermo Fisher Scientific, USA) in KIST.

2.10 Statistical analysis

Experiments were performed three times and data were presented as mean values \pm standard deviation (SD). All data of experiment were processed by the one-way ANOVA in SPSS program (IBM SPSS Statistics Version 24.0, IBM Consulting, USA) and p values < 0.05 were considered to be significant.

III. Results & Discussion

3.1 Physicochemical properties of nano-sized ethosome

The phospholipid nano vesicles were prepared by high pressure homogenization rather than traditional thin film hydration method. The mass ratio of the aqueous phase was higher than the oil phase, and formulation was in the liquid phase and had low viscosity. The prepared formulation had to be in the liquid phase in order to pass through the nano-disperser. The appearances of VAE #1 – 3 were pinkish and opaque, and VAE #4 – 6 containing 0.3 – 0.6 % ceramide were off-white as well as translucent (Fig 7 and 8). ABE' s appearances were off-white and had an opaque formulation overall. All ethosome samples were stored at 4, 25, or 45 °C for one month, and the particle size, zeta potential and polydispersity index were measured weekly. VAE #1 – 5 and ABE #1 – 6 were stable for a month at 25, 4, and 45°C, while VAE #6 with 0.6 % ceramide was unstable at 45 °C after one month. Those results were in good agreement with previous research. [22] Ethosomes with ceramide 0.6 % and biotin had similar stability over one month.

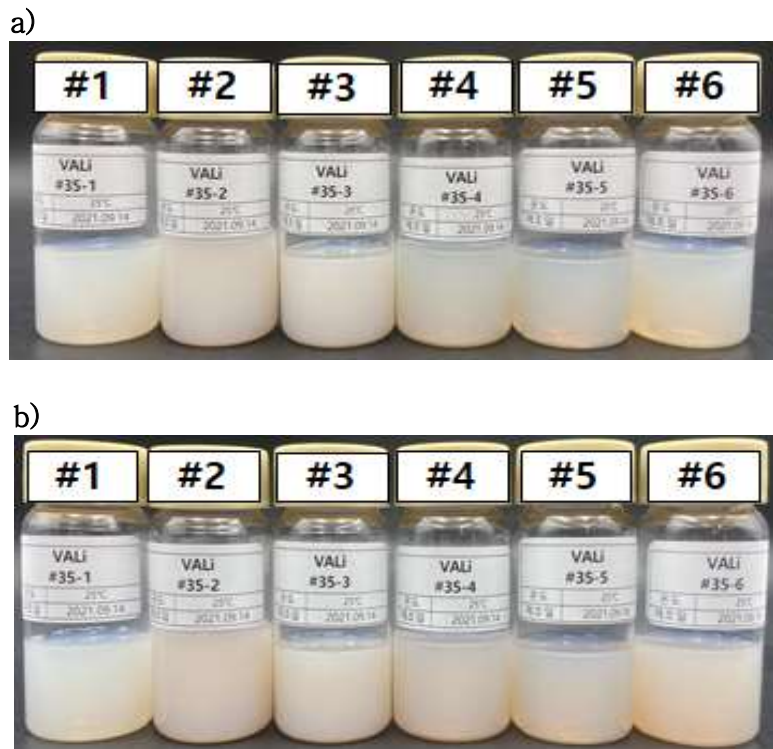


Fig 7. Appearance of VAE #1~6 at 25°C after (a) a day and (b) 4 weeks.

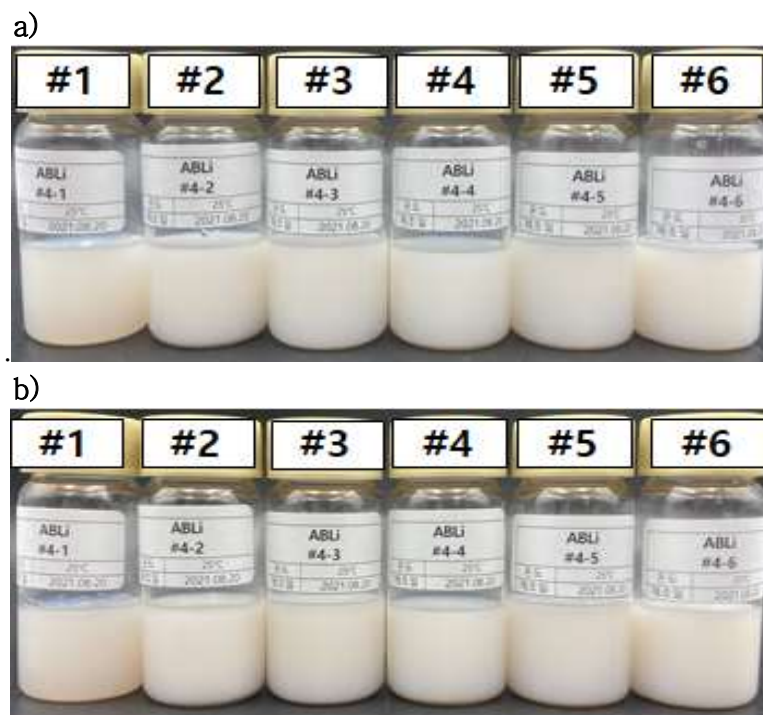


Fig 8. Appearance of ABE #1~6 at 25°C after (a) a day and (b) 4 weeks.

Table 5. Appearance, particle size, PDI, zeta potential of VAE, and ABE
(25°C, a day, mean ± SD, n=3)

No.	Feature	Appearance	Particle size (nm)	Polydispersity Index
VAE #1	CR, VA free	Off-white, Opaque	124.20 ± 1.25	0.209 ± 0.002
VAE #2	CR free	Pinkish, Opaque	121.27 ± 1.03	0.108 ± 0.006
VAE #3	0.15% CR	Pinkish, Opaque	138.23 ± 0.49	0.083 ± 0.018
VAE #4	0.3% CR	Pinkish, Translucent	97.28 ± 0.79	0.133 ± 0.009
VAE #5	0.45% CR	Pinkish, Translucent	86.12 ± 0.60	0.148 ± 0.012
VAE #6	0.6% CR	Pinkish, Translucent	82.46 ± 0.63	0.127 ± 0.005
ABE #1	CR, AB free	Off-white, Opaque	172.70 ± 1.55	0.226 ± 0.012
ABE #2	CR free	Off-white, Opaque	207.30 ± 1.35	0.233 ± 0.004
ABE #3	0.15% CR	Off-white, Opaque	183.23 ± 0.76	0.269 ± 0.002
ABE #4	0.3% CR	Off-white, Opaque	170.07 ± 0.74	0.288 ± 0.004
ABE #5	0.45% CR	Off-white, Opaque	180.07 ± 5.08	0.287 ± 0.011
ABE #6	0.6% CR	Off-white, Opaque	173.90 ± 4.42	0.273 ± 0.003

(CR = ceramide, VA = vanillic acid, AB = α -Bisabolol)

3.1.1 Particle size and polydispersity index of nano-sized ethosome in line with ceramide

Particle size and polydispersity index of ethosome with or without ceramide are compared in Fig 9. VAE #1 or ABE #1 was free drug and free ceramide ethosome, and #2 was only free ceramide ethosome. When compared #1 and #2, particle size of VAE containing hydrophilic drug was not drastically different, whereas that of ABE containing lipophilic drug was increased. The hydrophilic drug encapsulated in aqueous core did not impact on particle size. By contrast, it seems likely that lipophilic drug was interdigitated between phospholipid or protruded outwards from the plane of the bilayer leading to an increased particle size. [28]

In the case of VAE #3–#6 shown in Table 5, addition of more ceramide leads to gradual decrease of the vesicle size. The particle size of ABE was also decreased by adding ceramide, but the particle size did not change sharply if the amount of ceramide over 0.3 %. The smaller particle size is perhaps due to the ceramide sandwiched between the phospholipids in the bilayer structure pulling on the phospholipids, resulting in a rather narrow gap between them. [29]

Moreover, in general liposome or nano-liposome formulation the polydispersity index is lower than 0.3 value in the range from 0.0 to 1.0, and this is considered to be a homogeneous distribution (Fig 10). [30] It was found that the PDI of VAE and ABE was lower than 0.3. When comparing with VAE

#1 and VAE #2 - 6, PDI of VAE #2 - 6 was reduced, perhaps because entrapped bioactive materials attract phospholipid head groups. Thus, the particle size of most vesicles was similar and the polydispersity index values were lower than 0.2. Thus, the particle size of most vesicles was similar and the polydispersity index values were lower than 0.2. In addition, α -Bisabolol was encapsulated in lamellar structure of phosphatidylcholine. Though these phenomena caused the carrier's size to increase, the PDI of ABE was lower than 0.3. Also, it could be reckoned the dispersity of ABE were homogeneous properties.

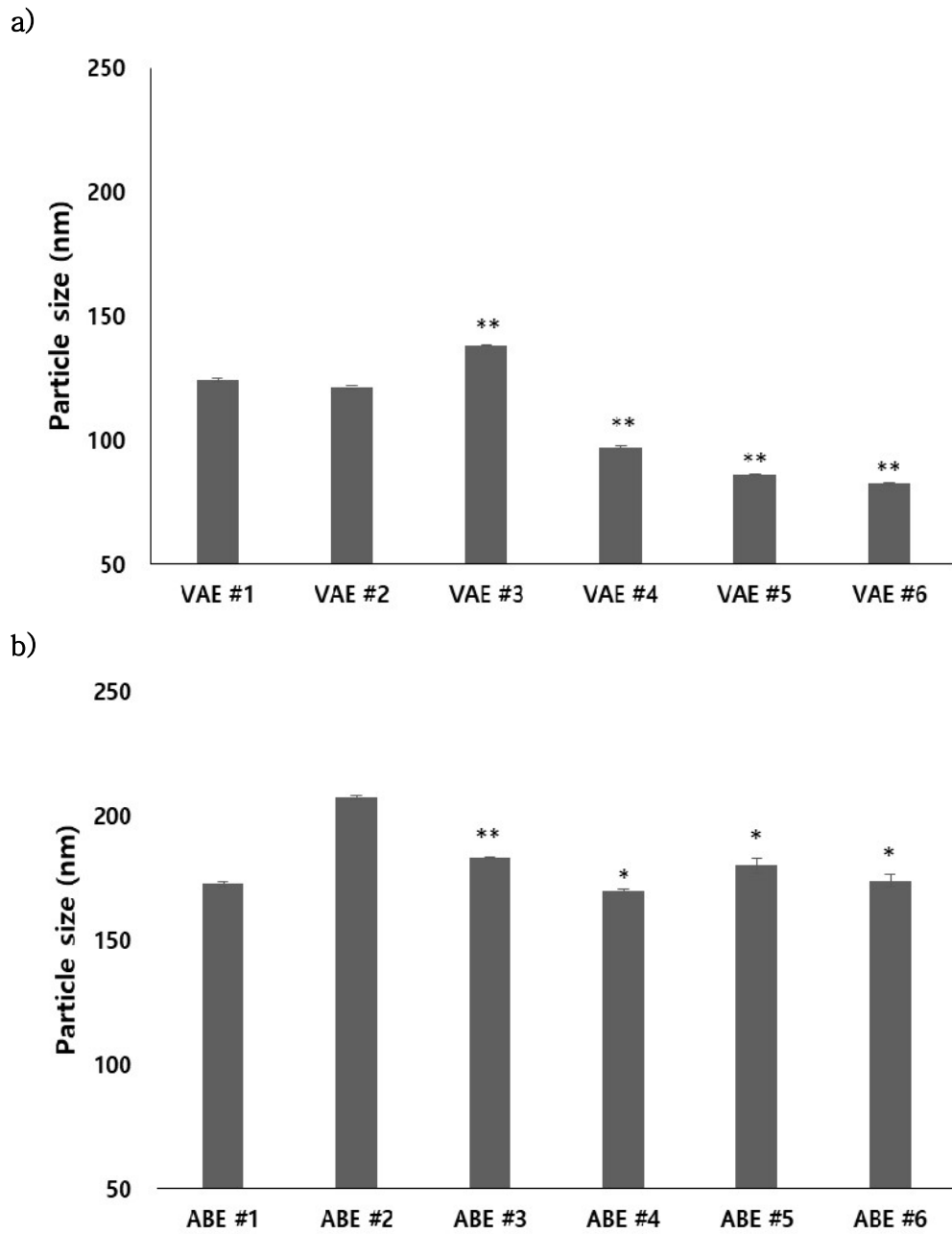


Fig 9. Particle size of (a)VAE and (b)ABE at 25°C after one day
(p-value * \leq 0.05, ** \leq 0.01, n=3)

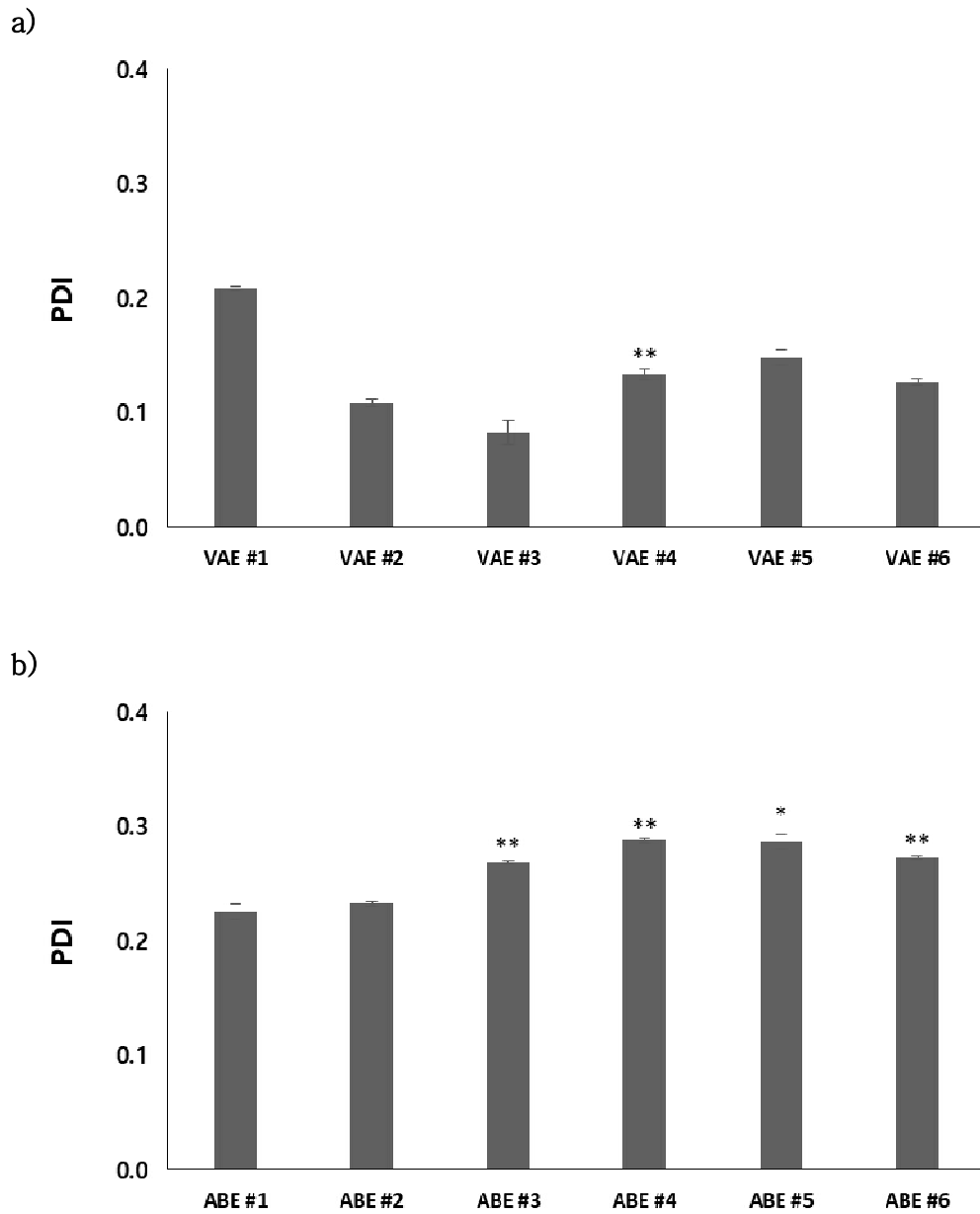


Fig 10. Polydispersity index of (a)VAE and (b)ABE at 25°C after one day (p-value * ≤ 0.05 , ** ≤ 0.01 , n=3)

3.1.2 Zeta potential of nano-sized ethosome in line with ceramide

The zeta potential provides an indication of particle stability. Zeta potential is electric force in the striping plane of particle. Repulsive force derived from zeta potential and attractive van der Waals act simultaneously between ethosome in the dispersion. This is designated the DLVO theory that named after Boris Derjaguin, Lev Landau, Evert Verwey, and Theodoor Overbeek. If the attraction is strong than repulsion, the particles aggregated. On the other hand, if the repulsive component is stronger than the attractive component, they will not aggregate. [31, 32] It has been reported that stability of the particulate is maintained when the absolute value of zeta potential is greater than 30 mV. [33] The graph of results of zeta potential were shown in Fig. 11. In the case of VAE #1, the vesicles did not contain any drug, the zeta potential value exceeded -60 mV, and the zeta potential of #2-#6 containing drug declined; however, they remained greater than -40 mV and could be considered stable. Free vanillic acid in ethosome dispersion led to a lowering of pH. Increasing positive charge induced by increasing concentration of hydrogen ion caused reduction of zeta potential. Inspection of variation of zeta potential between #2 and #6, implied that addition of ceramide did not play any role in the zeta potential of VAE. Besides, the zeta potential of ABE suggested that the particles were not disposed to aggregate, as the values were over -30 mV. The presence of α -Bisabolol in ethosomes had no effects on zeta potential. Presumably because the

molecule did not remain the aqueous part of dispersion but was entrapped in the phospholipid bilayer. Therefore, it remarkably demonstrated that unsubstantial variation of zeta potential brought about.

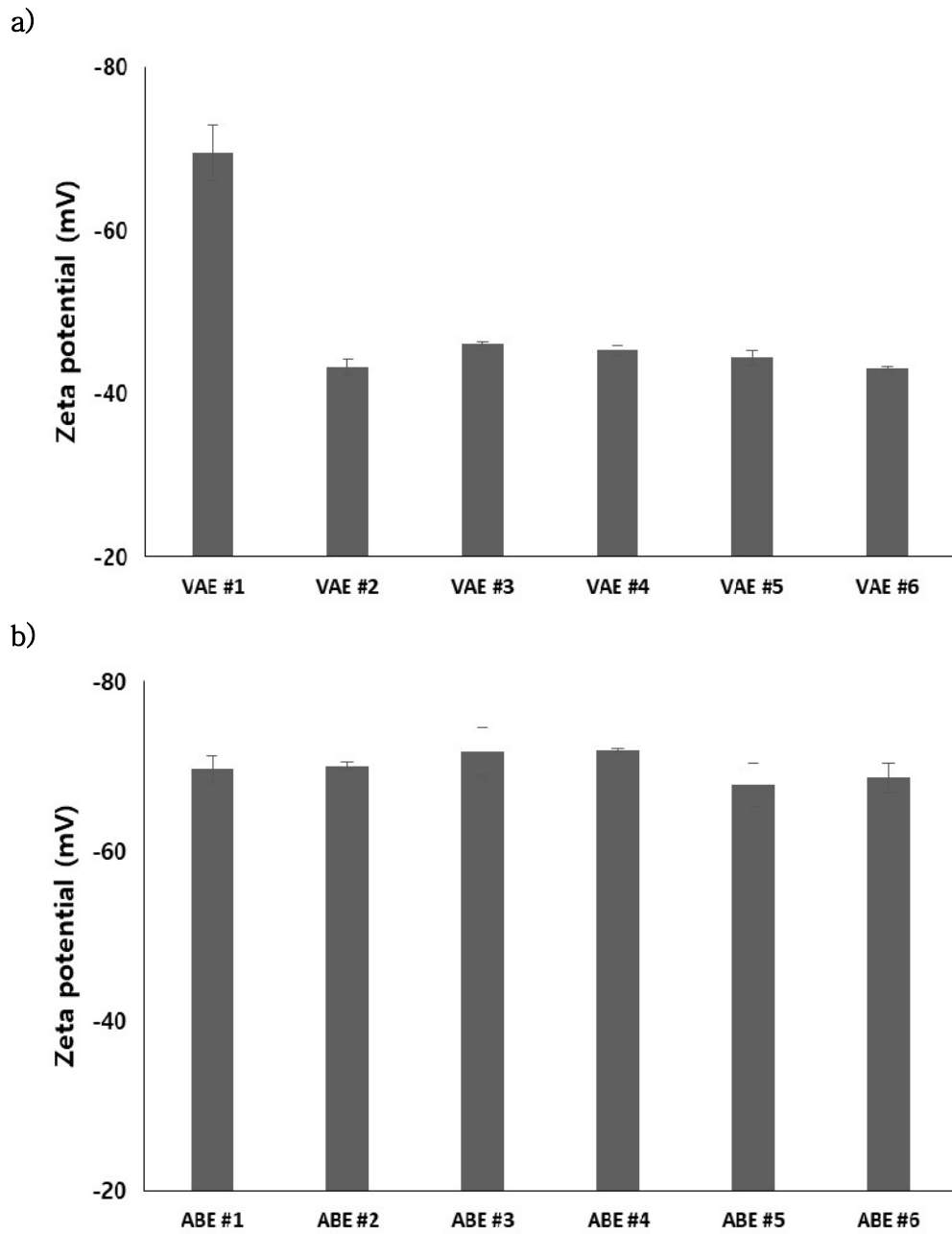


Fig 11. Zeta potential of (a)VAE and (b)ABE at 25°C after one day
 (p-value * ≤ 0.05 , ** ≤ 0.01 , n=3)

Table 6. Particle size (nm) of VAE and ABE over time (25°C, mean±SD, n=3)

No.	A day	1 week	2 weeks	3 weeks	4 weeks
VAE #1	124.20±1.25	123.43±0.61	124.13±0.40	123.0±1.21	123.57±0.31
VAE #2	121.27±1.03	123.53±0.85	124.97±1.44	126.80±1.31	127.97±0.95
VAE #3	138.23±0.49	139.27±0.55	139.00±0.10	139.77±1.48	139.90±0.52
VAE #4	97.28±0.79	101.87±0.57	98.92±0.53	101.17±0.38	103.80±0.72
VAE #5	86.12±0.60	88.35±0.67	89.31±0.52	89.98±0.79	91.04±0.20
VAE #6	82.46±0.63	85.18±0.97	89.74±0.39	93.74±0.59	100.59±1.00
ABE #1	172.70±1.55	172.90±2.00	173.93±1.10	171.20±1.47	173.40±1.54
ABE #2	207.30±1.35	218.20±1.25	234.73±2.44	240.90±2.10	244.13±0.95
ABE #3	183.23±0.76	192.77±1.97	194.40±1.73	206.23±0.92	197.80±2.00
ABE #4	170.07±0.74	173.10±1.35	190.50±5.20	183.47±1.72	187.67±1.91
ABE #5	180.07±5.08	162.73±1.76	167.33±0.60	167.20±0.30	168.13±0.67
ABE #6	173.90±4.42	171.87±2.12	172.83±2.12	172.83±2.12	179.73±1.21

Table 7. Polydispersity index of VAE and ABE over time (25°C, mean±SD, n=3)

No.	A day	1 week	2 weeks	3 weeks	4 weeks
VAE #1	0.209±0.002	0.214±0.004	0.215±0.012	0.222±0.012	0.227±0.005
VAE #2	0.108±0.006	0.098±0.002	0.098±0.016	0.088±0.012	0.088±0.022
VAE #3	0.083±0.018	0.053±0.029	0.080±0.019	0.079±0.024	0.080±0.010
VAE #4	0.133±0.009	0.184±0.022	0.129±0.006	0.122±0.012	0.125±0.017
VAE #5	0.148±0.012	0.132±0.012	0.144±0.017	0.130±0.017	0.112±0.021
VAE #6	0.127±0.005	0.123±0.007	0.144±0.009	0.196±0.005	0.276±0.026
ABE #1	0.226±0.012	0.229±0.008	0.245±0.007	0.244±0.009	0.230±0.009
ABE #2	0.233±0.004	0.265±0.005	0.279±0.006	0.305±0.005	0.310±0.015
ABE #3	0.269±0.002	0.269±0.008	0.260±0.011	0.273±0.010	0.265±0.008
ABE #4	0.288±0.004	0.277±0.002	0.287±0.008	0.267±0.008	0.277±0.017
ABE #5	0.287±0.011	0.270±0.003	0.253±0.011	0.256±0.007	0.264±0.010
ABE #6	0.273±0.003	0.264±0.005	0.258±0.005	0.258±0.005	0.268±0.005

Table 8. Zeta potential (mV) of VAE and ABE over time (25°C, mean±SD, n=3)

No.	A day	1 week	2 weeks	3 weeks	4 weeks
VAE #1	-69.43±5.92	-65.17±1.39	-62.83±0.45	-63.03±3.55	-58.27±2.75
VAE #2	-43.20±1.73	-44.97±0.99	-43.53±0.91	-45.80±0.30	-43.07±0.47
VAE #3	-46.07±0.40	-45.30±1.25	-45.63±0.75	-46.30±0.62	-46.90±1.39
VAE #4	-45.27±1.00	-45.73±1.71	-45.07±0.76	-46.70±0.70	-44.97±0.75
VAE #5	-44.37±1.53	-43.83±1.96	-44.23±0.59	-46.47±1.48	-46.70±0.30
VAE #6	-43.07±0.25	-45.60±1.30	-44.37±2.62	-42.07±0.71	-42.40±1.10
ABE #1	-69.67±2.73	-63.13±0.67	-71.10±2.35	-75.00±1.06	-66.57±0.84
ABE #2	-70.03±0.81	-66.30±2.23	-71.93±0.15	-72.10±2.17	-72.90±0.62
ABE #3	-71.73±4.96	-64.23±0.12	-71.93±1.39	-68.40±0.40	-69.87±1.80
ABE #4	-71.87±0.45	-65.00±0.95	-64.37±0.67	-69.73±0.83	-66.70±1.54
ABE #5	-67.77±4.41	-67.30±0.44	-72.60±4.20	-65.70±1.05	-68.10±1.04
ABE #6	-68.63±3.11	-67.73±1.10	-70.33±1.53	-67.00±1.05	-65.27±1.48

3.1.3 Particle size and polydispersity index of nano-sized ethosome over time

The particle size and PDI of phospholipid vesicles were measured after one, two, three and four weeks at 25 °C. Although the measured size of VAE and ABE was not changed drastically, variations of VAE #6 and ABE #2 showed a large difference compared with other samples (Table 6). It seemed likely that VAE #6 with ceramide 0.6% became unstable over time (Fig 12), and appeared to be unstable at 45 °C adjudged by changes in appearance. Picture of unstable appearance of that did not be inserted. Inspection of ABE #2 which did not contain ceramide, showed the particle size increased markedly the weeks went by. We surmised that α -Bisabolol containing ethosomes that lacked ceramide were inclined to fuse over time.

Furthermore, PDI of VAE #1 increased slightly and some others also changed (Table 7). The value of polydispersity index of VAE #6 was elevated for 4 weeks (Fig 13). The PDI of VAE #6 was 0.127 ± 0.005 after one day; however it increased to 0.276 ± 0.026 after 4 weeks. These differences of PDI implied that the ethosome stability was poor over the long term. Nevertheless, most of PDI of each samples were not higher than 0.3, suggesting that the ethosomes maintained a homogeneous formulation over time.

The polydispersity indices of ABE dispersions were not dynamically changed over time. Most of polydispersity index of ABE were lower than 0.3, whereas

the PDI of ABE #2 was greater than 0.3 after 3 weeks suggesting that ABE #2 became heterogeneous over time. Taken together, these results suggest that absence of ceramide has a destabilizing effect on ethosome structure.

To wrap up, we strongly suggests that the addition of ceramide into ethosome dispersion could have positive effects as well as minimal influences for the following reasons we mentioned above: for change of particle size, and polydispersity index.

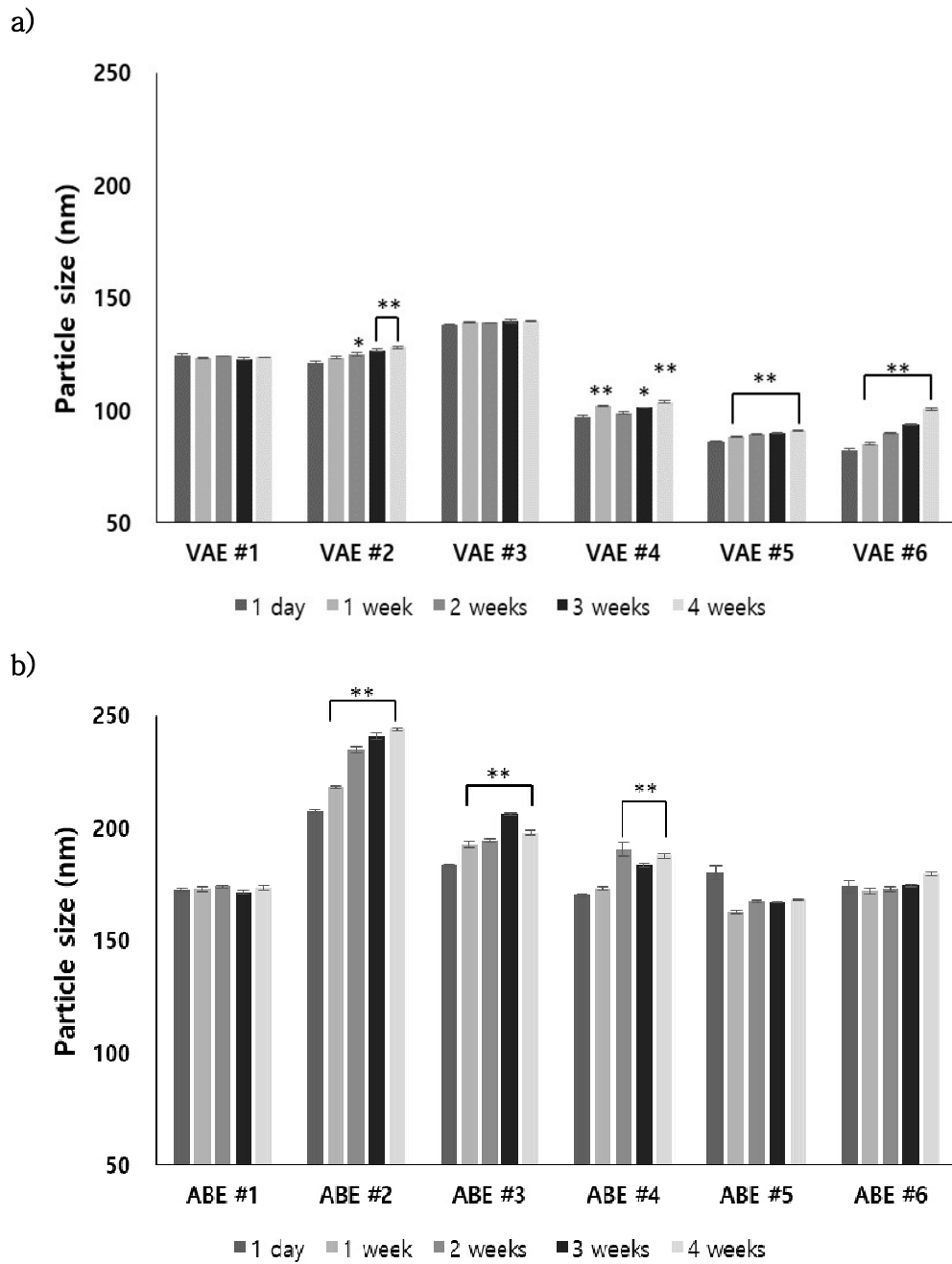


Fig 12. Particle size of (a)VAE and (b)ABE at 25°C over time
(p-value * ≤ 0.05 , ** ≤ 0.01 , n=3)

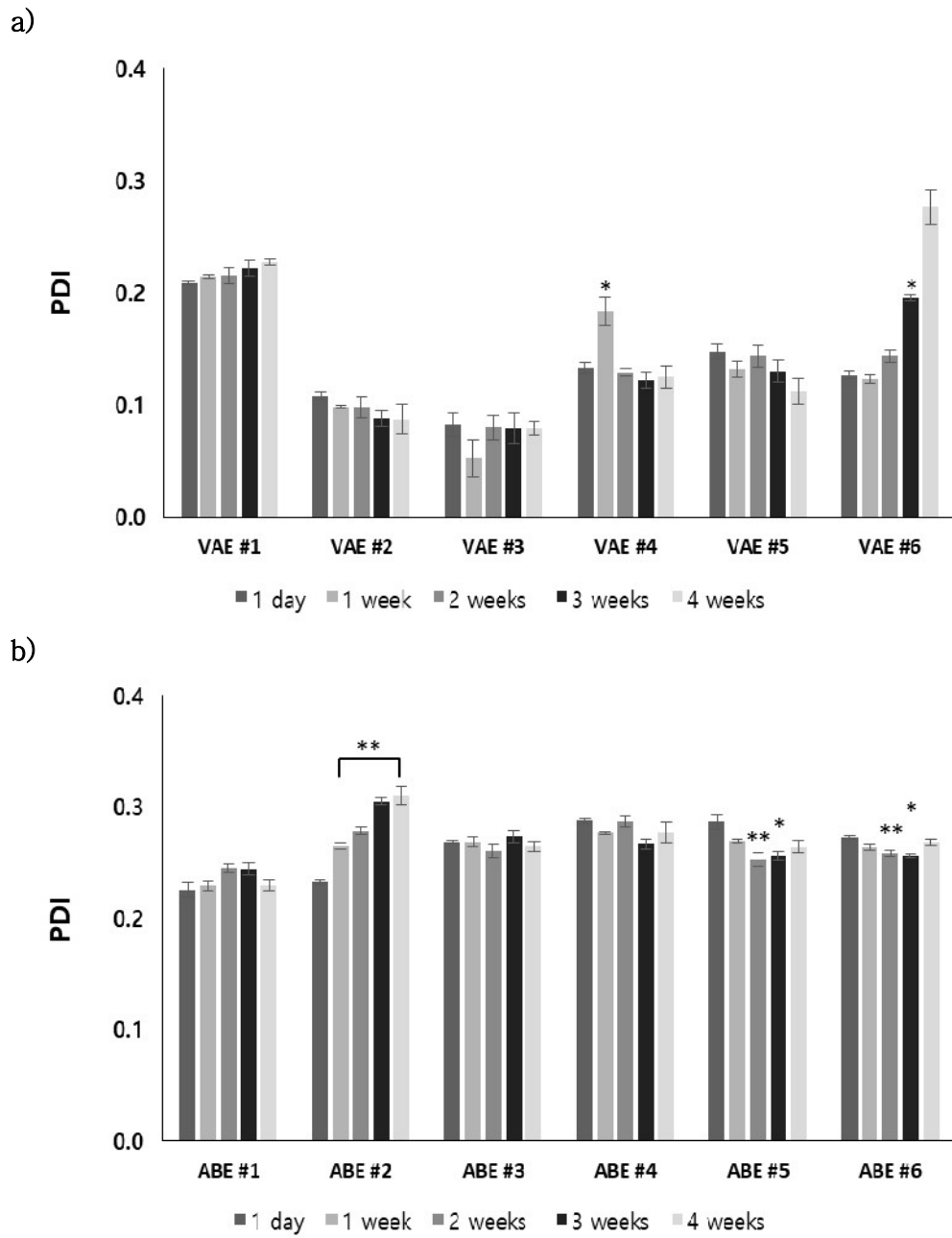


Fig 13. PDI of (a)VAE and (b)ABE at 25°C over time
(p-value * ≤ 0.05 , ** ≤ 0.01 , n=3)

3.1.4 Zeta potential of nano-sized ethosome over time

The zeta potential of bilayer lipid vesicles was measured after a day, a week, 2 weeks, 3 weeks, and 4 weeks in accordance with time. The graph of results were shown in Fig 14. The zeta potential measured weekly of VAE #2~#5 was higher than -40 mV and the observed variation did not change drastically (Table 8). Inspection of the data on the nano-sized vesicles containing ceramide, implied that the changes of zeta potential were not different compared with each sample. However, the value of zeta potential of ethosome without drug decreased over time in a drastic manner. The absolute difference of zeta potential between one day and 4 weeks of VAE #1 was 10 mV. On the contrary, the zeta potential of VAE #2-#6 after one day were as similar as after 4 weeks. Thus, the drug free ethosomes appear to be unstable over time.

In addition to VAE, the zeta potential of ABE did not show huge differences over time. Inserting ceramide into ethosomes had a slight influence on zeta potential. When observing the zeta potential of VAE #1 and ABE #1, the difference between the two samples was the presence or absence of L-arginine used as a neutralizing agent. Therefore, we inferred that the zeta potential was somewhat sensitive to the presence of L-arginine in the ethosome dispersion even though the actual amount of L-arginine was very small by weight.

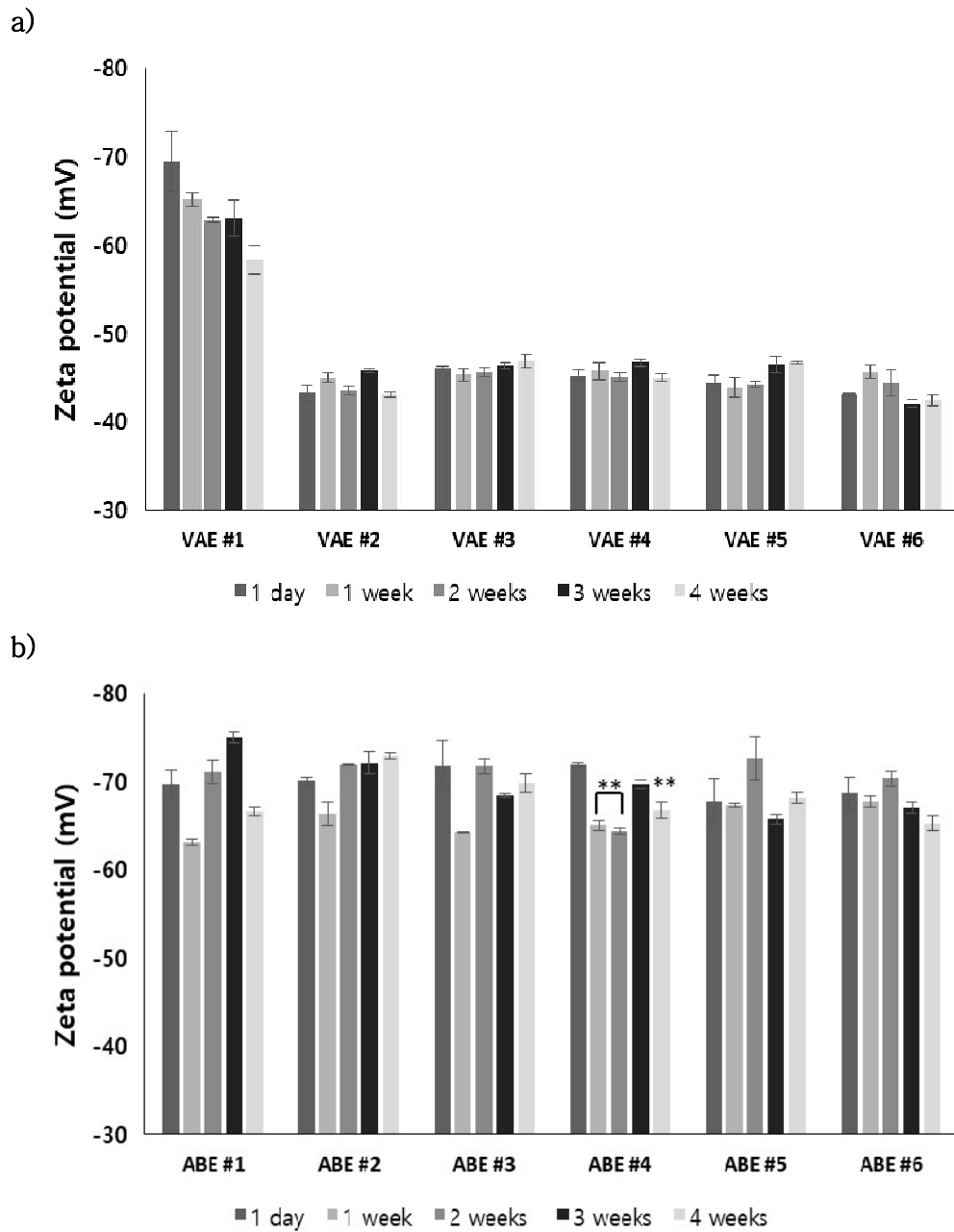


Fig 14. Zeta potential of (a)VAE and (b)ABE at 25°C over time
(p-value * ≤ 0.05 , ** ≤ 0.01 , n=3)

3.2 Skin absorption efficiency of nano-sized ethosome

The skin absorption efficiency was studied over 24 h at $37^{\circ}\text{C} \pm 1$ using a Franz diffusion-cell method. The sampling times were 1, 2, 4, 8, 12, and 24 h. After that, the amount of drug present in each samples was quantified by HPLC. The data are shown in Table 9 and 10, and the graph of skin absorption efficiency is given in Fig 15. It was observed that skin absorption efficiency of ethosome with vanillic acid and ceramide was increased compared with ethosome without ceramide. By contrast, the presence of ceramide slightly diminished skin absorption efficiency of ABE.

To begin with, when comparing vesicle containing ceramide with none ceramide vesicle, relatively higher percent of ceramide into ethosome improved the skin absorption efficiency. Specifically, the delivery ratio of VAE #6 was $23.57\% \pm 0.28$, VAE #4 was $22.82\% \pm 0.59$, and VAE #2 was $21.37\% \pm 0.47$ for 12h. If the weight ratio of ceramide was 0.6%, efficiency of drug carriers were boosted about 2% further than none ceramide ethosome. Moreover, by comparing with a non ethosome control formulation, nano-particulate carrier made it possible to enhance skin absorption. The ratio of it was higher than 5% for 12h, and 15% for 24 h. Thus, we surmised that it was likely the presence of ceramide in phospholipid bilayer carriers raised the skin absorption efficiency when studying ethosome with hydrophilic drug.

Meanwhile, although the skin absorption efficiency of VAE was elevated by the

addition of ceramide, it was not in the case of ABE. In other words, skin absorption efficiency of ABE #2 was $77.72\% \pm 0.70$, ABE #4 was $74.35\% \pm 0.16$, and ABE #6 was $72.23\% \pm 0.48$ for 24h. Increase in ceramide had pivotal influences on deterioration of transdermal. The results could be related to the encapsulation efficiency, and encapsulation of lipophilic drug and ceramide simultaneously caused the declining of skin absorption ability. A non-ethosome control was prepared from hydrogenated castor. Its skin absorption efficiency was lower 3–8% for 24h than ethanol vesicles. The case of lipid nano carriers with vanillic acid, however, was advanced results compared to control than ethosome with α -Bisabolol.

Table 9. Skin absorption efficiency (%) of VAE (37°C±1, mean±SD, n=3)

Time.	VAE#2	VAE#4	VAE#6	VAE control
1h	1.88±0.04	1.79±0.04	1.87±0.04	1.63±0.02
2h	3.96±0.08	3.97±0.09	4.14±0.10	3.72±0.14
4h	7.32±0.16	7.36±0.20	7.59±0.08	6.77±0.21
8h	13.37±0.36	13.96±0.42	13.97±0.25	11.99±0.35
12h	21.37±0.47	22.82±0.59	23.57±0.28	18.24±0.38
24h	78.96±0.78	80.89±1.64	71.51±0.38	56.37±0.48

Table 10. Skin absorption efficiency (%) of ABE (37°C±1, mean±SD, n=3)

Time.	ABE#2	ABE #4	ABE #6	ABE control
1h	2.75±0.07	2.90±0.04	2.73±0.06	5.93±0.03
2h	8.15±0.14	7.69±0.09	8.32±0.14	19.13±0.05
4h	23.62±0.27	22.46±0.14	23.41±0.19	39.12±0.31
8h	52.29±0.55	49.49±0.18	45.81±0.26	53.97±0.44
12h	64.72±0.65	59.57±0.12	58.56±0.37	60.62±0.59
24h	77.72±0.70	74.35±0.16	72.23±0.48	69.60±0.75

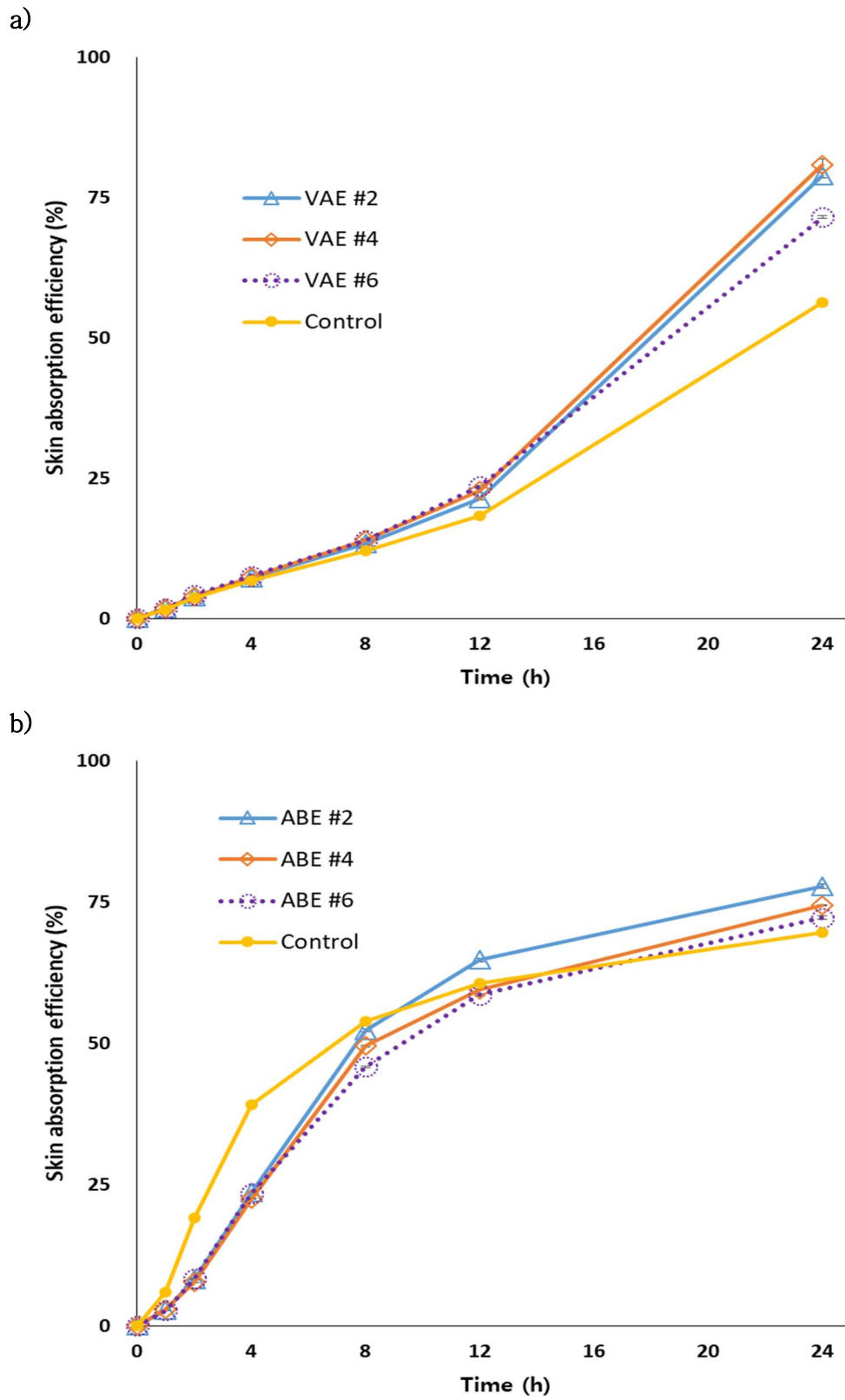


Fig 15. Skin absorption efficiency of (a)VAE and (b)ABE at $37^{\circ}\text{C} \pm 1$ ($n=3$)

3.3 Encapsulation efficiency of nano-sized ethosome

Before measuring the encapsulation efficiency of ethosome, each samples were segregated by centrifuge. Separated supernatant or remnant were analyzed by HPLC. It was expected that the encapsulation efficiency of ethosome by high pressure homogenization were lower than those produced by thin film hydration method. Phospholipid bilayer carriers prepared by high pressure homogenization were nano-sized vesicles and so the capacity to accommodate hydrophilic drugs in the aqueous core was smaller. [34] Also, the encapsulation efficiency of ABE#4 and #6 was expected to be lower than ABE #2 due to the presence of ceramide in the bilayer.

The encapsulation efficiencies of VAE overall were lower than 35%. The entrapment ratios of VAE #2, #4, and #6 were $21.63\% \pm 0.38$, $30.08\% \pm 1.81$, and 33.03 ± 1.28 . It checked out that VAE #6 was the highest encapsulation efficiency among them. The amount of phospholipid was limited, and the number of vesicles seemed to be similar; however, the number of vesicles were increased by adding ceramide. Thus, the encapsulation efficiency was risen. Although addition of ceramide supported increasing of encapsulation efficiency, the preparation method did not. In other words, high pressure homogenization method did not incorporate with evaporation of solvent, while the traditional thin film hydration method was included the solvent evaporation, and thus this step was known to help the high encapsulation efficiency rather than step of none

solvent evaporation.

Furthermore, the encapsulation efficiency of ABE varied with the amount of ceramide. From analysis of high performance liquid chromatography, the encapsulation efficiencies of ABE#2, ABE #4, and ABE#6 were $63.17\% \pm 0.36$, $46.58\% \pm 0.62$, and $43.52\% \pm 0.71$ respectively. The data are shown in Table 12. If the mass of ceramide is 0.3–0.6% (w/w) in the ethosome dispersion, the encapsulation efficiency was diminished because of less empty space of drug. It appeared likely that the ceramide competed with the α -Bisabolol for space between phosphatidylcholines.

3.4 Drug release of nano-sized ethosome

The drug release of particulate was studied by dialysis membrane method for 3 days at $37^{\circ}\text{C}\pm 1$. Free drug of ethosome dispersion and unstable formulation could pass through the dialysis tube. The solution for dialysis membrane method was a mixture of NaCl, PBS, water, and polysorbate 20. Polysorbate 20 as a surfactant was additionally put into solution for drug release of ABE. There are two types of graph in this paper. It was demonstrated (%) cumulative drug release vs time for 72 h and 12h in Fig 16 and 17.

The drug release of VAE #2 and #4 was fast, as 80% drug released through dialysis tube after 1 h. The data is shown in Table 13. After 4h, about 95% drug were evaded, while drug of VAE #6 kept running away for 72 h. The drug release of VAE #6 was $77.78\% \pm 0.27$ for 72 h. It intimated that VAE with 0.6% ceramide could have sturdy bilayer, so it revealed the slow drug release compared with others. Drug release of VAE #2 and VAE #4 was decreased after 8h, as it considered that the concentration of vanillic acid in the dialysis tube and it outside tube were equilibrating.

In addition to VAE, α -Bisabolol from drug release shown in Table 14. was not detected for 2h, while it was discovered after 4h. It is seemed likely that the quantity of drug release after 2h was so low that it was not detected. After 24h, the number of α -Bisabolol from ABE #2, #4, #6 were $77.12\% \pm 1.21$, $57.79\% \pm 1.35$, and $50.96\% \pm 0.28$ (Table 14). The drug of ABE #2 was released almost

after 24h, and other samples were also released over 78% after 48h (Fig 16). The drug release of three samples were over 85% after 72h. ABE #2 without ceramide were the highest rate of drug releases among them from this results. Thus, it was demonstrated that the sturdy of bilayer was not enough to grab bilayer for a long time due to absence of ceramide from outer stimulation.

Table 11. Encapsulation efficiency (%) of VAE (mean±SD, n=3)

	VAE#2	VAE#4	VAE#6
EE (%)	21.63±0.38	30.08±1.81	33.03±1.28

Table 12. Encapsulation efficiency (%) of ABE (mean±SD, n=3)

	ABE#2	ABE#4	ABE#6
EE (%)	63.17±0.36	46.58±0.62	43.52±0.71

**Table 13. Drug release (%) of VAE by dialysis membrane method
(37°C ± 1, mean±SD, n=3)**

Time.	VAE#2	VAE#4	VAE#6
1h	88.08±0.36	82.23±0.73	42.48±0.07
2h	94.25±0.29	94.66±0.56	48.41±0.24
4h	96.32±0.20	98.02±0.20	55.97±0.23
8h	95.34±0.36	97.37±0.36	64.04±0.23
12h	94.82±0.38	97.55±0.24	68.52±0.30
24h	95.45±0.37	96.18±0.19	68.52±0.30
48h	92.26±0.27	92.84±0.14	77.41±0.16
72h	89.06±0.68	92.63±0.24	77.78±0.27

**Table 14. Drug release (%) of ABE by dialysis membrane method
(37°C ± 1, mean±SD, n=3)**

Time.	ABE#2	ABE#4	AB#6
1h	0.00±0.00	0.00±0.00	0.00±0.00
2h	0.00±0.00	0.00±0.00	0.00±0.00
4h	2.33±2.02	1.10±0.63	1.14±0.65
8h	22.36±1.44	13.52±1.08	13.59±0.05
12h	38.60±0.97	25.16±0.54	23.71±0.58
24h	77.11±1.21	57.79±1.35	50.96±0.28
48h	84.15±0.97	80.16±0.50	78.09±1.12
72h	88.44±0.64	86.19±1.82	85.54±0.75

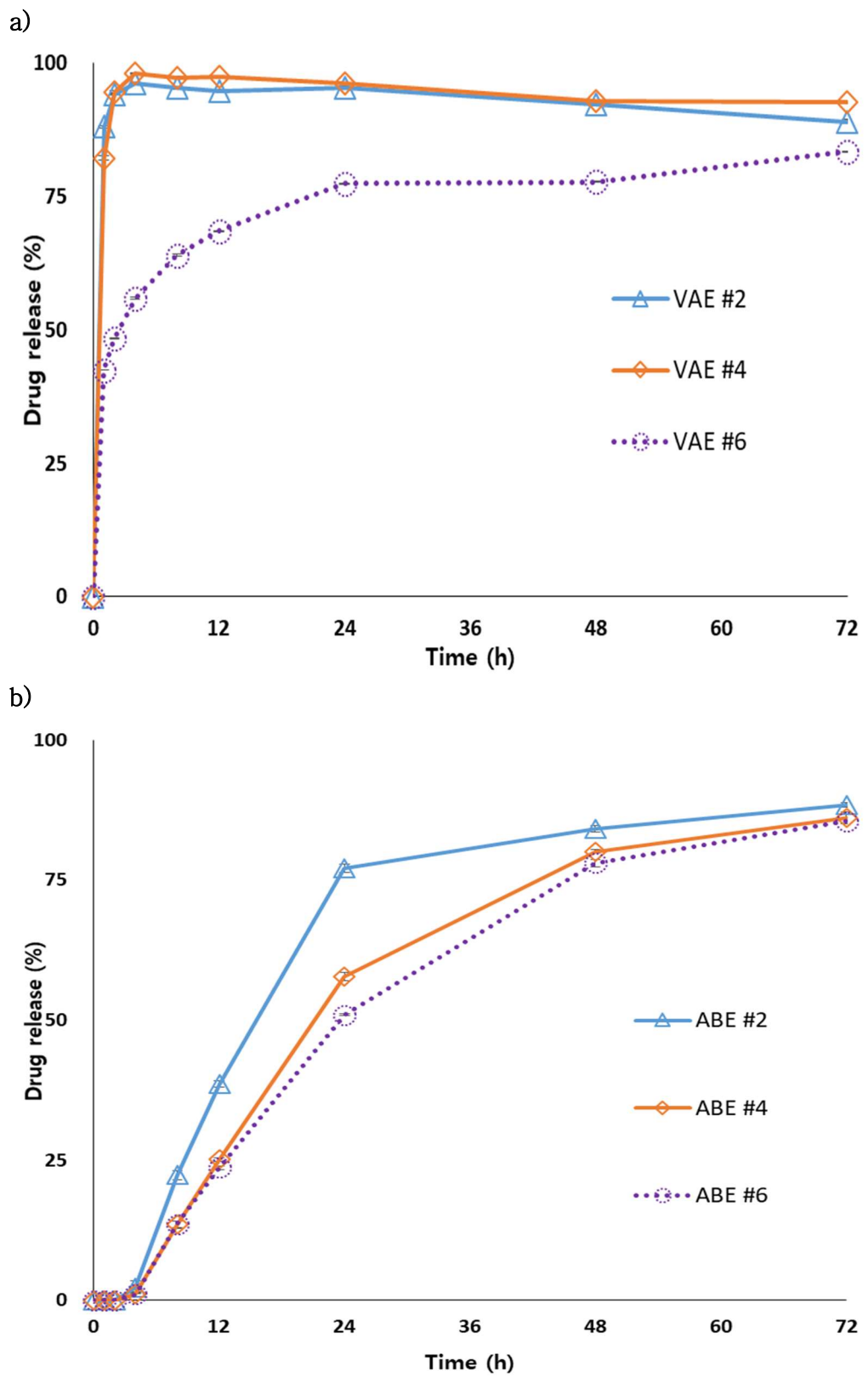


Fig 16. Drug release of (a)VAE and (b)ABE at $37^{\circ}\text{C}\pm 1$ by dialysis membrane method for 72 h. (n=3)

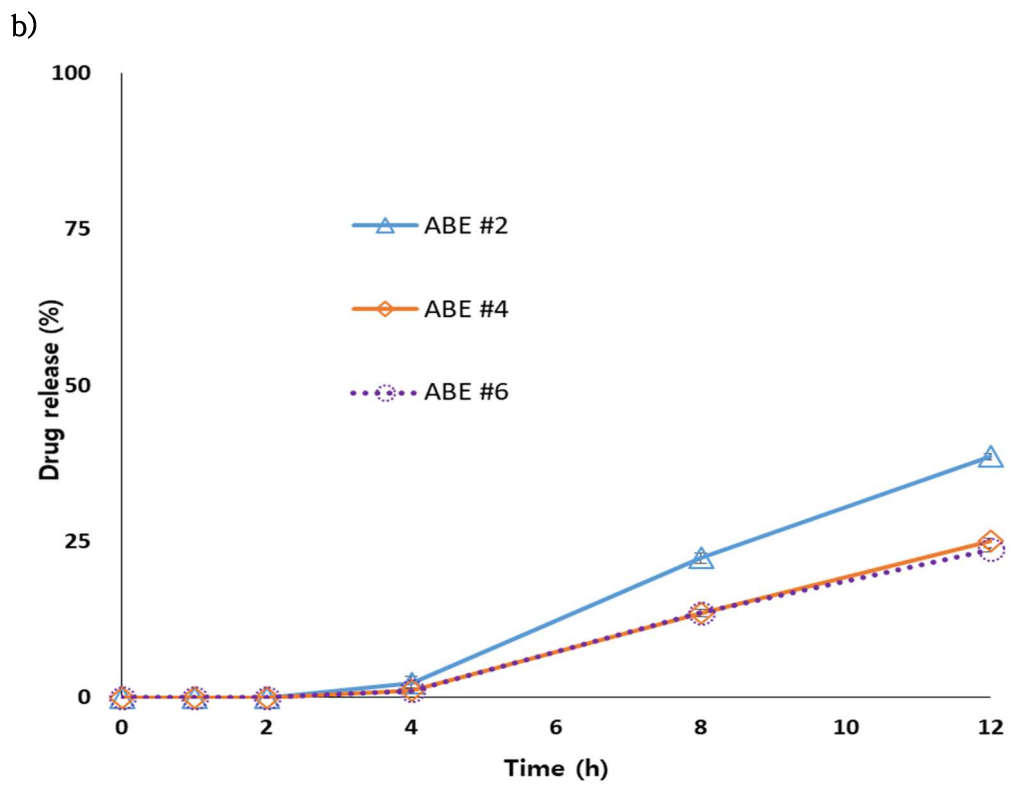
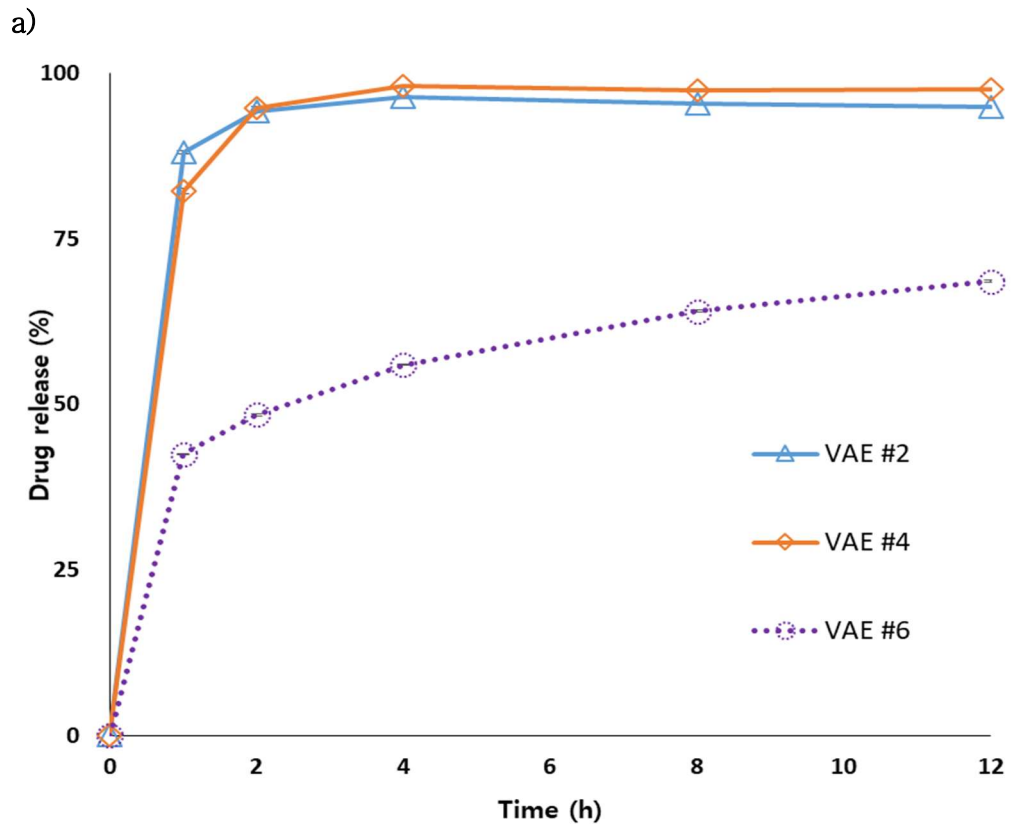


Fig 17. Drug release of (a)VAE and (b)ABE at $37^{\circ}\text{C}\pm 1$ by dialysis membrane method for 12 h. (n=3)

3.5 Cryo-TEM image of nano-sized ethosome

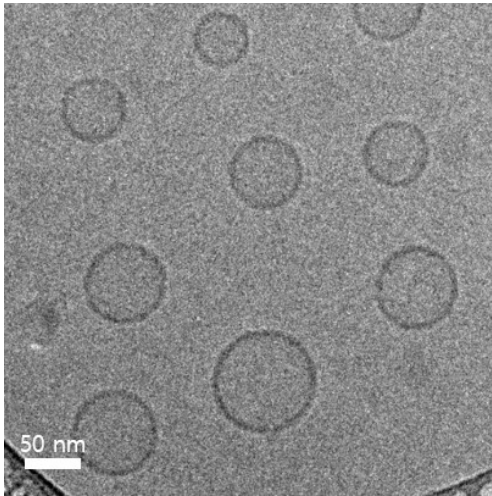
I inevitably commissioned morphology photograph of ethosome to KIST (Korea Institute of Science and Technology, Korea), and particle of ethosome was analyzed by cryo transmission electron microscope. The photo samples were VAE #6 and ABE #6 which were containing ceramide 0.6%. Photos of VAE #6 and ABE #6 were shown in Fig 18 and 19. The morphologies of VAE #6 were spherical structures and the range of particle size was about 50 ~ 100 nm (Fig 18. a, b). Through the TEM image, it indicated that the particle of VAE #6 was small unilamellar vesicles, or SUV. Thought the primary ethosome dispersion was passed two time through nano-disperser, a multilamellar vesicle was found in the Fig 18. c. It seemed likely that two pass number of time by nano-disperser was not enough to completely convert large multilamellar vesicles to small unilamellar vesicles. However, it was quite difficult to find large multilamellar vesicles due to so low the number of it among vesicles.

Furthermore, the TEM image of ABE #6 illustrated that the vesicles were large unilamellar vesicles, as the range of particle size was 150 ~ 200 nm. The vesicles that was lower than 50 nm were oval shape instead of spherical form. These particle size was too small to be constructed globular shape as well as the cranny of between phospholipids was too close. (Fig 19. a, b) [35] Also, by considering the encapsulation efficiency of ABE #6, the other

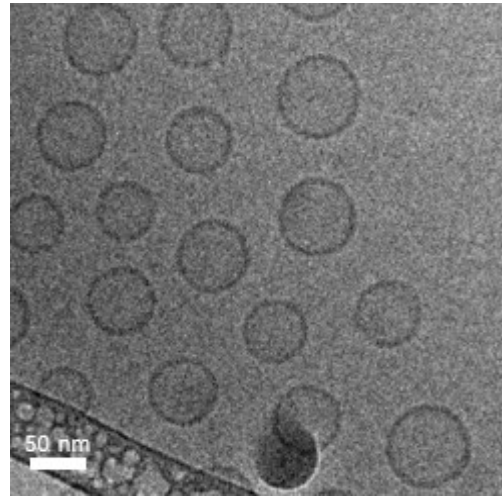
formulations were existed. The encapsulation efficiency of ABE #6 was 43.52% in Table 12. The α -Bisabolol is an oil ingredient, and then it cannot exist in the aqueous part. Thus, in Fig 19 b and c, it seems likely that the formulation without dark layer is an emulsion formulation rather than ethosome. [36]

In addition to vesicles, it was suspicious that the disc were discovered in the right side of Fig 19. c. It was considered that the pretreatment of samples before detecting cryo-TEM could be caused the disc shape. The TEM shot the electron beam to the vesicles, and it was probably that nano-carreirs were damaged from electron beam.

a)



b)



c)

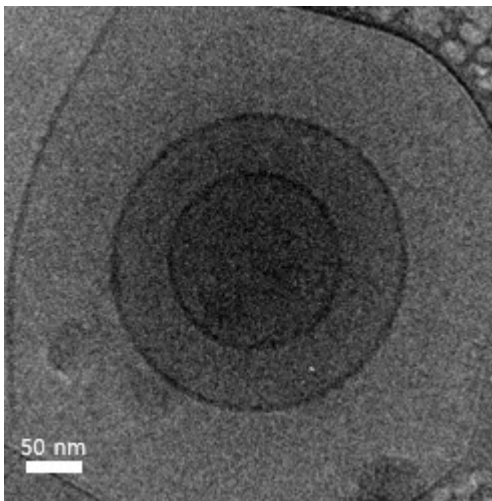
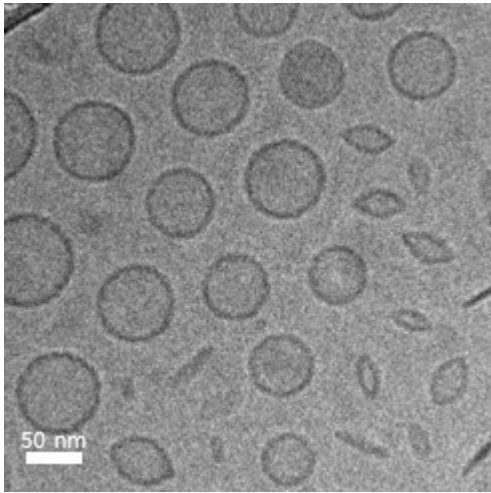
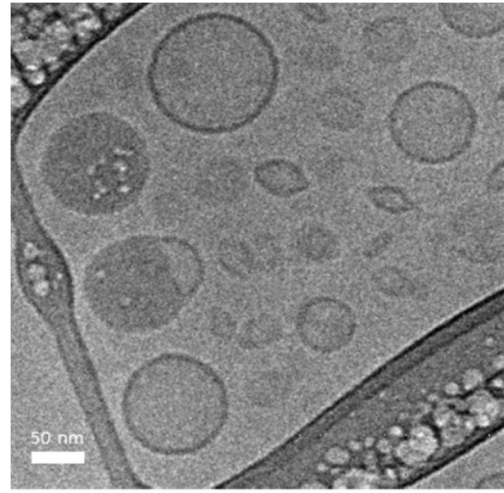


Fig 18. Cryo-TEM image of VAE #6

a)



b)



c)

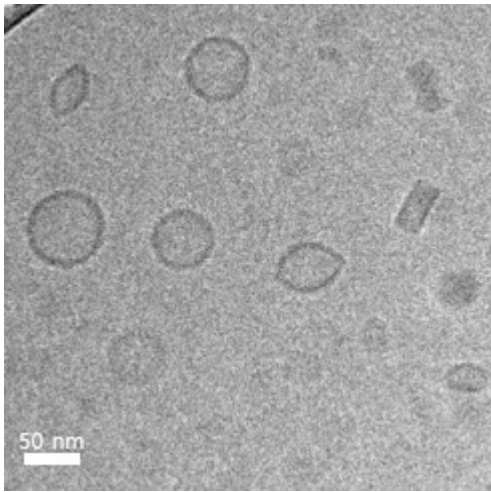


Fig 19. Cryo-TEM image of ABE #6

IV. Summary & Conclusion

In this research, physicochemical properties of ethosome in accordance with ceramide and drugs were studied in order to develop cosmetic formulation. The phospholipid nano particulate carriers prepared by nano disperser were stored at 4, 25, and 45°C for a month. By utilizing DLS and electrophoresis, particle size, polydispersity index, and zeta potential were measured. The skin absorption efficiency by Franz diffusion cell, encapsulation efficiency, and drug release by dialysis membrane method were analyzed by HPLC. The morphology of vesicles was imaged by cryo-TEM at KIST.

The presence of ceramide was shown diminishing of particle size in VAE, while the similar results were not found in ABE. The particle size of VAE were tinier than ABE, as VA was located in where aqueous core in the ethosome, whereas AB in bilayer structure. It was checked out that polydispersity index of most samples were lower than 0.3, and zeta potential were higher than absolute 40 mV. It suggested that VAE and ABE were homogeneous and stable nano particles from several pieces of evidence. Ethosome with hydrophilic drug and ceramide had improved skin absorption efficiency, whereas case of lipid bilayer particle with lipophilic drug and ceramide faintly worsened. This is because hydrophobic drug cannot escape

from competition with ceramide, and then these brought about lower encapsulation efficiency of ABE #4 and ABE #6. As a results, it alluded that the falling of encapsulation efficiency deteriorated skin absorption efficiency to epidermal system. The drug release of VAE was faster than ABE due to difference of encapsulation efficiency. VAE #6 and ABE #6 with ceramide 0.6% had lower drug release compared with other samples. This is because ceramide grab the phospholipid in the bilayer and the sturdy of ethosome became stronger. By collecting cryo-TEM images, the ethosome formulation was existed as small unilamellar vesicles, oval shape and sparsely multi lamellar vesicles.

Overall, it was proved that addition of ceramide into ethosome had several advancements. The advantages of addition ceramide into ethosome with hydrophilic drug improved decrease of particle size, higher encapsulation efficiency, and more stable formulation. Also, lipophilic drug ethosome with ceramide could be delivered simulataneously without great difference of skin absorption efficiency. Therefore, we suggests that the ethosome with ceramide could be availed itself of the cosmetic industry.

V. Acknowledgement

This research was financially supported by the Ministry of Trade, Industry and Energy, Korea, under the "Regional Innovation Cluster Development Program(R&D, P001529)" supervised by the Korea Institute for Advancement of Technology(KIAT).

VI. Reference

- [1] G. M. El Maghraby, B. W. Barry, A. C. Williams, Liposomes and skin: From drug delivery to model membranes, *Eur. J. Pharm. Sci*, 2008, 34, 203–222
- [2] J. Hadgraft, Skin, the final frontier, *Int. J. Pharm.*, 2001, 224, 1–18
- [3] H. Trommer, R. H. H. Neubert, Overcoming the stratum corneum: the modulation of skin penetration, *Skin. Pharmacol. Physiol.*, 2006, 19, 106–121
- [4] G. Betz, A. Aeppli, N. Menshutina, H. Leuenberger, In vivo comparison of various liposome formulations for cosmetic application. *Int. J. Pharm.*, 2005, 296, 44–54
- [5] J. S. Dua, A. C. Rana, A. K. Bhandari, Liposome: Methods of Preparation and Applications, *Int. J. Pharm. Sci. Res.*, 2012, 3(2), 14–20
- [6] S. kaddaha, N. Khreich, F. Kaddah, C. Charocosset, H. Greige–Gerges. Cholesterol modulates the liposome membrane fluidity and permeability for a hydrophilic molecule. *Food. Chem. Toxicol.*, 2018, 113, 40–48
- [7] J. M. Lopez–Pinto, M. L. Gonzalez–Rodriguez, A. M. Rabasco, Effect of cholesterol and ethanol on dermal delivery from DPPC liposomes. *Int. J. Pharm.*, 2005, 298(1), 1–12
- [8] A. D. Bangham, M. M. Standish, G. Weissmann, The action of steroids and streptolysin S on the permeability of phospholipid structures to cations,

- J. Mol. Biol., 1965, 13(1), 253–259
- [9] D. T. Birnbaum, J. D. Kosmala, D. B. Henthorn, L. Brannon–Peppas, Controlled release of β –estradiol from PLGA microparticles: The effect of organic phase solvent on encapsulation and release, J. Control. Release., 2000, 65, 375–387
- [10] P. Verma, K. Pathak, Therapeutic and cosmeceutical potential of ethosomes: An overview, J. Adv. Pharm. Tech. Res., 2010, 1(5), 274–282
- [11] E. Touthou, N. Dayan, L. Bergelson, B. Godin, M. Eliaz. Ethosomes–novel vesicular carriers for enhanced delivery: characterization and skin penetration properties. J. Control. Release., 2000, 65, 403–418
- [12] R. Kadir, B. W. Barry, α –Bisabolol, a possible safe penetration enhancer for dermal and transdermal therapeutics, Int. J. Pharm., 1991, 70(1–2), 87–94
- [13] N. F. M. Rocha, E. R. V. Rios, A. M. R. Carvalho, G. S. Cerqueira et al, Anti–nociceptive and anti–inflammatory activities of (–)– α –Bisabolol in rodents, Naunyn–Schmiedeb. Arch. Pharmacol., 2011, 384(6), 525–533
- [14] P. S. M. Prince, S. Rajakumar, K. Dhanasekar, Protective effects of vanillic acid electrocardiogram, lipid peroxidation, antioxidants, proinflammatory markers and histopathology in isoproterenol induced cardiotoxic rats, Eur. J. Pharmacol., 2011, 668, 233–240
- [15] J. Kang, J. Moon, E. Kim, Y. Lee, Y. K. E. Yoo, H. Kang, D. Yim, The

- Hair Growth Effects of Wheat Bran, *Kor, J, Pharmacogn.*, 2013, 44(4), 384–390
- [16] S. J. Kim, M. C. Kim, J. Y. Um, S. H. Hong, The beneficial effect of vanillic acid on ulcerative colitis, *Molecules.*, 2010, 15, 7208–7217
- [17] M. Rabionet, K. Gorgas, R. Sandhoff, “Ceramide synthesis in the epidermis” , *Biochim. Biophys. Acta. Mol. Cell. Biol. Lipids.*, 2014, 1841(3), 422–434
- [18] L Cui, Y Jia, Z. W. Cheng, Y. Gao, G. L. Zhang, J. Y. Li, C. F. He, Advancements in the maintenance of skin barrier/skin lipid composition and the involvement of metabolic enzymes, *J. Cosmet. Dermatol.*, 2016, 15, 549–558
- [19] S. L. Chamlin, J. Kao, I. J. Frieden, M. Y. Sheu, A. J. Fowler, J. W. Fluhr, M. K. Willams, P. M. Elias, Ceramide–dominant barrier repair lipids alleviate childhood atopic dermatitis: changes in barrier function provide a sensitive indicator of disease activity, *J. Am. Acad. Dermatol.*, 2002, 47, 198–208
- [20] M. Brandil, D. Bachmann, M. Drechsler, K. H. Bauer, Liposome preparation by a new high pressure homogenizer gaulin micron lab 40, *Drug. Dev. Ind. Pharm.*, 1990, 16(14), 2167–2191
- [21] N. Sharma, S. Mishra, S. Sharma, R. D. Deshpande, R. K. Sharma, Preparation and optimization of nanoemulsions for targeting drug delivery, *Int. J. Drug Dev. & Res.*, 2013, 5(4), 37–48
- [22] T. I. Hyeon, K. S. Yoon, Skin absorption and physical property of

- ceramide-added ethosome, *Journal of the Korean applied science and technology*, 2021, 38(3), 801–812
- [23] N. Ostrowsky, Liposome size measurements by photon correlation spectroscopy, *Chem. Phys. Lipids.*, 1993, 64(1–3), 45–56
- [24] M. N. Trainer, P. J. Feud, E. M. Leonardo, High-concentration submicron particle size distribution by dynamic light scattering, *Am. Lab.*, 1992, 24(11), 34–39
- [25] Z. Zhang, Y. Wo, Y. Zhang, D. Wang, R. He, H. Chen, D. Cui, In vitro study of ethosome penetration in human skin and hypertrophic scar tissue, *Nanomedicine.*, 2012, 8(6), 1026–1033
- [26] H. J. Gwak, B. S. Jin, Preparation and Characterization of EGCG Entrapped Ethosome, *J. Korean. Ind. Eng. Chem.*, 2007, 18(2), 130–135
- [27] C. K. Kim, M. H. Min, K. H. Min, W. R. Lah, B. J. Lee, Y. B. Kim, Synthesis of N-Stearyl lactobionamide(N-SLBA) and preparation of Neo-galactosylated liposome, *Yakhak Hoeji.*, 1992, 36(2), 159–166
- [28] A. Zeb, S. T. Arif, F. A. Shah, F. U. Din, O. S. Qureshi, E. S. Lee, G. Y. Lee, J. K. Kim, Potential of nanoparticulate carriers for improved drug delivery via skin, *J. Pharm. Investig.*, 2019, 49, 485–517
- [29] A. Overbye, A. Holsaeter, M. Fusser, N. Skalko-Basnet, T. Inversen, M. Lyngass Torgersen, T. Sonstevold, O. Engebarraten, K. Flatmark, G. M. Maelandsmo, T. Skotland, K. Sandvig, “Ceramide-containing liposomes with doxorubicin: time and cell-dependent effect of C6 and C12 ceramide”, *Oncotarget.*, 2017, 8(44), 76921–76934

- [30] M. Danaei, M. Dehghankhold, S. Ataei, F. H. Davarni, R. Javanmard, A. Dokhani, S. Khorasani, M. R. Mozafari, Impact of particle size and polydispersity index on the clinical applications of lipidic nanocarrier systems, *Pharmaceutics.*, 2018, 10(2), 57–73
- [31] B. Derjaguin, L. Landau, Theory of the stability of strongly charged lyophobic sols and of the adhesion of strongly charged particles in solutions of electrolytes, *Prog. Surf. Sci.*, 1993, 43(1–4), 30–59
- [32] E. J. W. Verwey, J. Th. G. Overbeek, Theory of the stability of lyophobic colloids, *J. Colloid. Sci.*, 1995, 10(2), 224
- [33] A. laouini, C. Jaafar–Maalej, I. Limayem–Blouza, S. Sfar, C. Charcosset, H. Fessi, Preparation, characterization and applications of liposomes: state of the art, *J. Colloid. Sci. Biotechnol.*, 2012, 1(2), 147–168
- [34] E. Abd, J. Gomes, C. C. Sales, S. Yousef, F. Forouz, K. C. Telaprolu, M. S. Roberts, J. E. Grice, P. S. Lopes, V. R. Leite–Silva, N. Andreo–Filho, Deformable liposomes as enhancer of caffeine penetration through human skin in a Franz diffusion cell test, *Int. J. Cosmet. Sci.*, 2021, 43, 1–10
- [35] J. Kuntsche, J. C. Horst, H. Bunjes, Cryogenic transmission electron microscopy (cryo–TEM) for studying the morphology of colloidal drug delivery systems, *Int. J. Pharm.*, 2011, 417, 120–137
- [36] V. Klang, N. B. Mastsko, C. Valenta, F. Hofer, Electron microscopy of nanoemulsions: An essential tool for characterization and stability assessment, *Micron*, 2012, 43, 85–103